(TRC-50IX; Topcon Corporation, Tokyo, Japan). For FA, photographs were taken after the injection of 0.075 mL/kg of 10% sodium fluorescein solution (Fluorescite; Alcon Japan Ltd., Tokyo, Japan) into a vein.

D. Electroretinography

Bright-light flash electroretinograms (ERG) were recorded 1 month after the implantation of the STS electrode array. Under general anesthesia with pupil dilation, corneal contact lens electrode/LED mini-Ganzfeld stimulator (WLS-20; Mayo Corporation, Nagoya, Japan) was used for ERG recording. The animal was dark-adapted for 30 minutes before the ERG recordings. Responses elicited by bright flash stimuli were amplified, band pass filtered from 0.5 to 1000 Hz, and digitized at 3.3 kHz. Five responses were averaged.

E. Functional Testing of STS System

The voltage in the microelectronic circuit of the decoder was monitored by an external circuit. The maximum voltage of this circuit was 10.0 V, and we set 9.5 V as a saturation voltage. Just after and at 1month after implantation, we checked to be sure that the voltage did not exceed the saturation voltage of 9.5 V. Each of the 49 electrodes was activated with balanced, cathodic-first biphasic pulses of up to 1000 uA, with a duration of 0.5 ms/phase and pulse duration of 0.5 ms. The frequency of the pulses was 20 Hz for 0.5 seconds that was controlled by the extraocular stimulator driven by the external transmitter. If the voltage in the electric circuit in the microstimulator was less than the saturation voltage, the device set the current as pass, but if the voltage exceeded the saturation voltage, the device set the current as failure. Next the artifacts evoked by electrical stimulation were recorded with a contact lens corneal electrode/LED mini-Ganzfeld stimulator (WLS-20; Mayo Corporation).

III. Results

A. Implantation Surgery

All prostheses were safely implanted and no intraoperative complications occurred. The electrode array was inserted in the scleral pocket without bleeding (Fig. 2) and the multiplexer attached with electrode array was kept stably under the conjunctiva. The cable was flexible and encircled the globe. No sign of infections or wound dehiscence was observed.

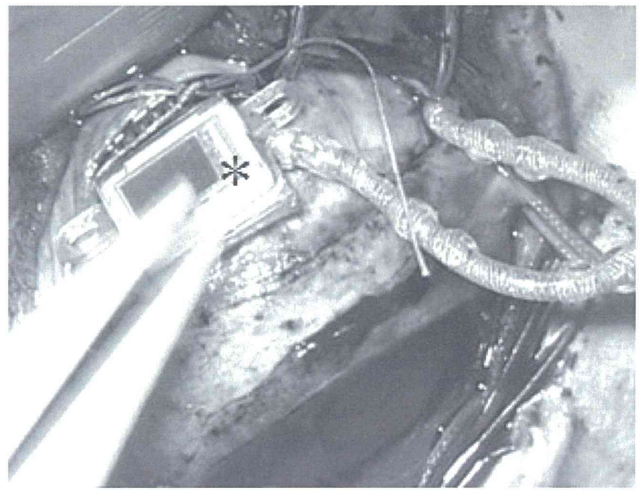

Figure2. Photograph taken during implantation surgery. An electrode array was inserted into the scleral pocket, and the multiplexer was sutured (*) to the sclera. Asterisk mark indicates the multiplexer.

B. Postoperative ocular fundus

Fundus photographs of the two dogs showed that the implanted electrode array was not detectable, and there was no obvious indication of surgical damage or side effects. FA showed intact vasculature without signs of inflammation, leakage, obstruction, or formation of new vessels in the area overlying and surrounding the implant in all dogs.

C. Electroretinography

The electroretinograms had normal a-wave and b-waves, and the shapes did not differ from those of electroretinograms recorded from the unoperated fellow eye 1 month after implantation in all two animals. (Fig. 3)

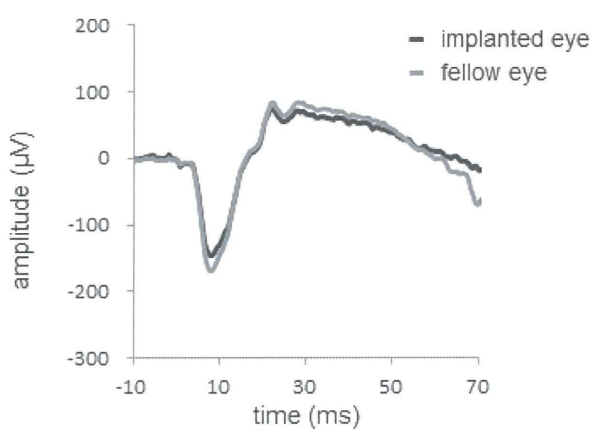

Figure 3. Representative electroretinograms recorded of the implanted eye and fellow eye of dog 1 after one month implantation.

D. Functional Testing of STS System

The voltage in the microelectronic circuit of the decoder was less than the saturation voltage in all electrodes and in all cases throughout the observation period. Representative stimulus artifact waveforms recorded with a contact lens electrode are shown in Figure 4. All the electrodes could deliver the electric currents.

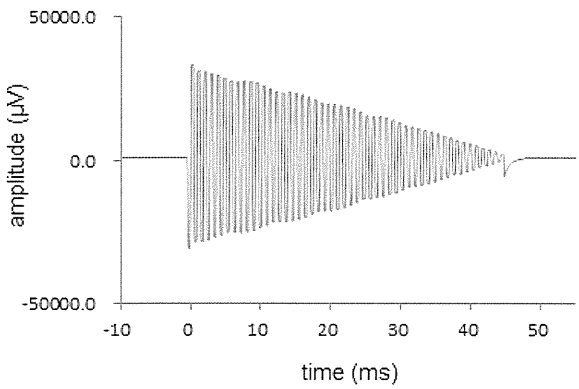

Figure 4. Representative waveforms of the stimulus artifacts of dog 1. Drawing of the waveforms of artifacts derived from each of 49 electrodes sequentially. Amplitudes of artifacts increase with increasing current intensity.

IV. Discussion

Our results showed that it is possible to implant our 2nd generation STS device into the scleral pocket of beagle dogs without intraoperative or postoperative complications.

The device were consisted of 49 channel electrode array with multiplexer and a decoder with internal coil. The device was different from that of 1st generation in that multiplexer was added to deliver electrical pulses to each 49 channel electrodes without increasing the number of lead wires.

The multiplexer have 5.7 × 4.4 mm in area and set close (10.5 mm) to the corneal limbs, so a possibility exists that the device is exposed from the conjunctiva if the friction between the lid and conjunctiva is increased. However the multiplexer was covered by the conjunctiva stably for 1 month, suggesting that the new device is able to be implanted stably in human trial.

The new device equipped a junction between the decoder and the lead wires, so a possibility exists to disconnection between the device and wires. However, the device was functional 1 month after the implantation, suggesting that the new device is kept functional at least 1 month.

Further observation is necessary to confirm the long-time safety and efficacy of our 2nd generation STS retinal prosthesis.

V. Conclusion

The 2nd generation STS system with a 49 channel electrode array is implanted successfully in 2 dogs. One month after surgery, all electrodes were functioning and the ocular fundus was normal in both dogs, suggesting that the 2nd generation STS retinal prosthesis is feasible and can be considered for clinical use.

Acknowledgment

The authors thank their project partners Kouji Oosawa, Eiji Yonezawa, Yasuo Terasawa, and Tohru Saitoh (Vision Institution, Nidek Co., Ltd.) for the development of new devices.

References

[1] M.F. Marmor, G .Aguirre, G .Arden, et al., "Retinitis pigmentosa: a symposium on terminology and methods of examination," Ophthalmology, vol. 90, pp. 126-131, 1983.

[2] R.A.Pagon, "Retinitis Pigmentosa," Surv Ophthalmol, vol. 33, pp. 137-177, 1988.

[3] Margalit E, Maia M, Weiland JD, Greenberg RJ, Fujii GY, Torres G, Piyathaisere DV, O'Hearn TM, Liu W, Lazzi G, Dagnelie G, Scribner DA, de Juan E Jr, and Humayun MS, "Retinal prosthesis for the blind," Surv Ophthalmol, vol. 47, pp. 335-356, 2002

[4] Zrenner E, "Will retinal implants restore vision?," Science, vol. 295, pp. 1022-1025, 2002

[5] Chader GJ, Weiland J, and Humayun MS, "Artificial vision: needs, functioning, testing of a retinal electronic prosthesis," Verhaagen et al (Eds.) , Progress in Brain Research, vol. 175, pp. 317-332, 2009.

[6] Fujikado T, Kamei M, Sakaguchi H, Kanda H, Morimoto T, Ikuno Y, Nishida K, Kishima H, Maruo T, Konoma K, Ozawa M, and Nishida K, "Testing of Semi-chronically Implanted Retinal Prosthesis by Suprachoroidal-Transretinal Stimulation in Patients with Retinitis Pigmentosa, " Invest Ophthalmol Vis Sci., vol. 52, pp. 4726-33, 2011.

[7] Morimoto T, Kamei M, Nishida K, Sakaguchi H, Kanda H, Ikuno Y, Kishima H, Maruo T, Konoma K, Ozawa M, Nishida K, and Fujikado T, "Chronic implantation of newly developed suprachoroidal-transretinal stimulation (STS) prosthesis in dogs," Invest Ophthalmol Vis Sci., vol. 52, pp. 6785-92, 2011.

Experimental Eye Research 109 (2013) 1–7

Contents lists available at SciVerse ScienceDirect

Experimental Eye Research

journal homepage: www.elsevier.com/locate/yexer

Optical imaging of retina in response to grating stimuli in cats

Y. Hirohara [a,c], T. Mihashi [b], H. Kanda [c], T. Morimoto [c], T. Miyoshi [d], J.S. Wolffsohn [e], T. Fujikado [c,*]

[a] Optical Engineering Laboratory, Topcon Corp., Itabashi, Japan
[b] Innovative Research Initiatives, Tokyo Institute of Technology, Japan
[c] Department of Applied Visual Science, Osaka University Graduate School of Medicine, Suita, Osaka, Japan
[d] Department of Physiology, Osaka University Graduate School of Medicine, Suita, Japan
[e] School of Life and Health Sciences, Aston University, Birmingham, UK

ARTICLE INFO

Article history:
Received 19 November 2012
Accepted in revised form 11 January 2013
Available online 24 January 2013

Keywords:
retina
intrinsic signal
light stimulation
grating
spatial frequency
MTF
wavefront aberration

ABSTRACT

We examined the intrinsic signals in response to grating stimuli in order to determine whether the light-evoked intrinsic signals of the retina are due to changes in the photoreceptor activities induced by the image projected on to the retina or are due to neural activities of the inner retina. The retinas of the left eye of 12 cats under general anesthesia were examined by a functional imaging fundus camera. Near infrared light was used to monitor the reflectance changes (RCs) of the retina. Vertical grating were used to stimulate the retina at 4 Hz. The spatial frequencies of the gratings were 0.05, 0.11, 0.22, 0.43, 0.86, 1.73, and 3.46 cycles/degree (cpd). Ten images were averaged and used to analyze the RCs to obtain the peak value (PV) of a two dimensional fast Fourier transfer of the RCs. The wavefront aberrations (WA) were measured with a compact wavefront aberrometer and the spatial modulation transfer function (MTF) of the eye was calculated. The retinal reflectance image had a grating pattern. The PV of the spatial sensitivity curve was highest at low spatial frequencies (0.05 and 0.11 cpd), and the sensitivity decreased steeply with an increase in the spatial frequency. RCs were not detectable at 3.46 cpd. The MTF decreased gradually with increases in the spatial frequencies and was 0.68 at 3.46 cpd. The reflectance pattern of the retinal intrinsic signal elicited by grating stimuli of different spatial frequencies was different from that of the MTF. This suggests that the intrinsic signal represents not only the response of the photoreceptors but also other neuronal or vascular changes in the retina.

1. Introduction

The processing of visual signals by the retina has been extensively investigated by electrophysiological methods. Thus, single unit recordings from retinal ganglion cells (RGCs) showed that the spatial sensitivity of the retina had a band-pass shaped curve which is the result of lateral inhibition (Enroth-Cugell and Robson, 1966). The lateral inhibition is believed to be due to either horizontal cells in the outer retina or to amacrine cells in inner retina or by both (Cook and McReynolds, 1998). Pattern ERGs elicited by pattern reversal stimuli arise because of non-linear informational processing in the retina (Ohzawa and Freeman, 1985; Sieving and Steinberg, 1987; Fujikado, 1994). However, *en face* analyses of retinal information processing have not been reported.

In experimental myopia studies, it was hypothesized that hyperopic blur will cause a progression of myopia while myopic blur will not (Smith et al., 2005). However, the neural activity of RGCs recorded *in vitro* does not respond differently to hyperopic and myopic blur (Diedrich and Schaeffel, 2009). So, a more global estimation method is needed to investigate how retinal information processing is altered under different blur conditions.

Functional imaging of the retina was recently developed to analyze the reflectance changes induced by light or electrical stimulation (Crittin and Riva, 2004; Inomata et al., 2008; Okawa et al., 2007; Schallek et al., 2009b). After light stimulation, the reflectance changes have been reported to be caused mainly by the photoreceptors (Schallek et al., 2009b). However, the reflectance changes in the retina following electrical stimulation of the chiasma was completely suppressed by an intravitreal injection of tetrodotoxin (Mihashi et al., 2011). Therefore, it was concluded that there must be some contribution of the inner retinal layers to the intrinsic signals (Hanazono et al., 2008).

Recently, Li et al. (2010) reported that the intrinsic optical signal elicited by visible light from *ex vivo* frog retinas is recorded not only

* Corresponding author. Tel.: +81 6879 3941; fax: +81 6 6879 3458.
E-mail address: fujikado@ophthal.med.osaka-u.ac.jp (T. Fujikado).

0014-4835/$ – see front matter © 2013 Elsevier Ltd. All rights reserved.
http://dx.doi.org/10.1016/j.exer.2013.01.007

in the photoreceptor layer but also in the inner plexiform and ganglion cell layer. They also showed that intrinsic signal in the photoreceptor layer was confined to the area of light stimulation, while that of inner layers spread from the stimulus site into relatively large area. The study suggests that intrinsic signals might represent the information processing in inner layers of the retina.

The purpose of this study was to determine the reflectance changes evoked by grating stimuli of different spatial frequencies. To accomplish this, we stimulated the retina with gratings of different spatial frequencies and determined the modulation transfer function (MTF) of the eyes of cats. From these findings, we determined whether the reflectance changes were due to the optical properties of the eye or to retinal information processing.

2. Methods

2.1. Animals

Twelve cats were studied. They were initially injected intraperitoneally with atropine sulfate (0.1 mg/kg), and after 30 min, they were anesthetized with an intramuscular injection of ketamine hydrochloride (25 mg/kg). The anesthesia was maintained by a continuous intravenous infusion of pentobarbital sodium (1 mg/kg/h). The cats were paralyzed by infusion of pancuronium bromide (0.2 mg/kg/h) mixed with Ringer's solution and glucose (0.1 g/kg/h).

The animals were artificially ventilated with a mixture of N_2O/O_2 (1:1), and the end-tidal CO_2 concentration was controlled at 3.5–5.0% by altering the frequency and tidal volume of the ventilation. The intratracheal pressure and electrocardiogram were also monitored. The body temperature was maintained at 38 °C with a heating pad.

All experiments were performed in accordance with the ARVO Statement for the Use of Animals in Ophthalmic and Visual Research, and the procedures were approved by the Animal Research Committee of the Osaka University Medical School.

2.2. Surgical procedures

To prevent eye movements, a stainless steel ring was sutured to the sclero-corneal limbus, and the ring was fixed to a stereotaxic head holder. The pupil was dilated with 5% phenylephrine hydrochloride, 0.5% tropicamide, and 1% atropine sulfate. To protect the corneal surface, a hard contact lens (polymethylmethacrylate; base curve, 8.50 mm; power, +1.5 diopters; diameter, 13.5 mm) was placed on the cornea.

2.3. Optical imaging of reflective changes of retina

The apparatus used for the optical imaging is diagrammed in Fig. 1. The ocular fundus was monitored by a fundus camera (TRC-50LX, Topcon Corp. Tokyo, Japan) with a digital CCD camera (C8484, Hamamatsu Photonics, Hamamatsu, Japan). The number of pixels of the camera was 1280 × 1024. A 12-bit digitizer was used, and a 4096 grayscale was set for each pixel. The exposure time of the CCD images was 40–79 ms.

A halogen lamp was used to illuminate the posterior fundus, and 3 band pass filters were inserted in the optical path to limit the wavelength from 730 to 770 nm, 780 to 820 nm, or 830 to 880 nm (Fig. 1). This pathway was used to monitor the reflectance changes of the retina.

The power of the monitor light was 250 nW which was much lower than the safe exposure limit decided by American National Standard Institute. To reduce the background fluctuations of the light power, a stabilized power supply (PS-150UE-DC, Hayashi Watch Works) was used. All experiments were performed in a dark room after 60 min of dark-adaptation.

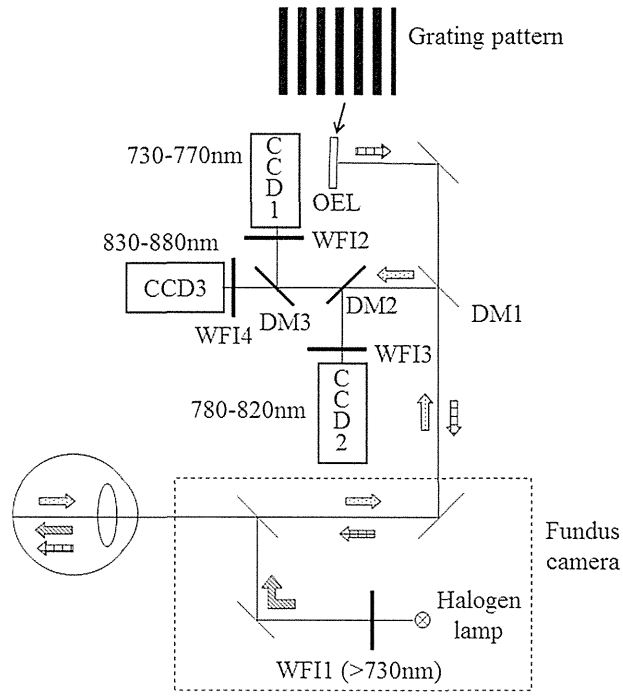

Fig. 1. Schematic diagram of functional-imaging fundus camera using 3 different wavelengths. A digital CCD camera is used to photograph the fundus with 3 different wavelengths nearly simultaneously. Light from a halogen lamp is filtered (WFI1) and illuminates the fundus with a wavelengths longer than 730 nm. The light passing to the fundus is reflected by the first dichroic mirror (DM1) which reflects light with a wavelength of 730–880 nm. The second dichroic mirror (DM2) reflects light with a wavelength 780–820 nm and passes other infrared light. The third dichroic mirror (DM3) reflects light with a wavelength 730–770 nm and passes other infrared light. Three CCDs record the images with filters which passed 730–770 nm (WFI2), 780–820 nm (WFI3), 830–880 nm (WFI4). Rectangular gratings with 7 different spatial frequencies were generated by organic electroluminescent diode (OEL) and projected onto the retina.

2.4. Light stimulation

The grating with spatial frequencies of 0.05, 0.11, 0.22, 0.43, 0.86, 1.73, and 3.46 cycles/degree (cpd) were obtained from an organic electro luminescence (OEL) panel. Black and white gratings on a black background were used to stimulate the retina at 4 Hz for 4 s. The power of the stimulating light was 30 nW and the area of a projected image on the retina was 50*50°.

2.5. Measurement sequence

Images were obtained every 100 msec for 26 s, 2 s recording without stimulation, followed by 4 s recording with stimulation, and then 20 s recording without stimulation. The measurement was repeated 10 times at a rate of once/75 s.

2.6. Wavefront analyses

The wavefront aberrations of 6 eyes of 6 cats (Cats 7–12) that were also used for the optical imaging studies were analyzed by a custom-made wavefront sensor (Topcon) with a diameter of 2 mm at the center of pupil. The measured wavefront aberrations were Fourier transformed to obtain the point spread function which was then used to obtain the modulation transform function

(MTF). The MTF was squared to account for the inward and outward passage of the light.

2.7. Data analyses

To improve the signal-to-noise ratio, 10 images of 10 consecutive measurements were averaged with a speed of 10 frames/sec. To evaluate the intensity of the reflectance changes, two-dimensional images of the optical signal were obtained by subtracting the first image from all the subsequent recorded images. We evaluated the intensity of the reflectance changes by 2-dimensional fast Fourier transformation (2D FFT). The peak value of the spatial frequency of the vertical gratings in the horizontal profile of the FFT was selected to determine the time course (Fig. 2).

2.8. Statistical analyses

For the statistical analyses of the peak values, the values were normalized by the total gray scale value of the image. A two-way repeated measures ANOVA was performed to obtain the R value, and a P value ≤ 0.05 was taken to be significant.

3. Results

3.1. Wavefront analyses

The average root mean square (RMS) value of the wavefront aberration was 0.09 ± 0.03 μm (±SD) with a range from 0.04 to 0.12 μm. The MTF was 0.68 at 3.46 cpd, and it decreased monotonically with an increase in the spatial frequency (Fig. 3).

MTF calculated by optical system of the fundus camera and the combined MTF of the eye and the fundus camera were also shown in Fig. 3. The combined MTF showed that the value was 0.55 at 3.46 cpd, suggesting that gratings can be resolved on the retina by the optical system of the fundus camera.

3.2. Time course of 2D-FFT

In Fig. 4, typical images of the reflectance change in the retina in response to grating stimuli of 0.11 and 0.86 cpd with different ranges of wavelength are shown. Grating patterns were observed in both spatial frequencies and the frequency corresponded to that of stimulation.

A typical time course of the changes of the peak value is shown in Fig. 5 for Cat 4. The peak value started to increase at about 0.7 s and was maximal at about 4 s after the onset of light stimulation and then gradually decreased. The time course was similar for all spatial frequencies and for different wavelengths of light stimulation.

The maximum of the peak value was significantly higher for shorter wavelengths at all spatial frequencies (Table 1), and the time between the onset of stimulation and the maximum value, the implicit time, was not significantly different for the different wavelengths at all spatial frequencies (Table 1).

3.3. Spatial frequency dependence of 2D-FFT

The relationship between the peak value of the 2D-FFT and the spatial frequencies for all cats is shown in Fig. 6. For the shortest wavelengths (730–770 nm), the maximum of the peak value was highest at the lowest spatial frequency (0.05 cpd), and it decreased steeply with an increase in the spatial frequency in Cats 2, 3, 4, 5, 7, 8, 11. However in Cats 9, 10, and 12, the curve had a band-pass pattern and peaked at 0.11 cpd. The response pattern to the longer wavelengths was similar to that of the 730–770 nm group.

The average peak value decreased monotonically in the short and middle wavelength groups and had a band-pass pattern for the long wavelength group (Fig. 7).

4. Discussion

The reflectance changes of a grating imaged on the upper part of the retina where the tapetum exists is shown in Fig. 2. The time course of the changes in the peak value in the 2D FFT profile (Fig. 5) was similar to that of the reflectance changes after stimulation by a bar of light (Okawa et al., 2007; Schallek et al., 2009b). These findings would then indicate that the peak value represents the intrinsic signal in response to the light stimulation.

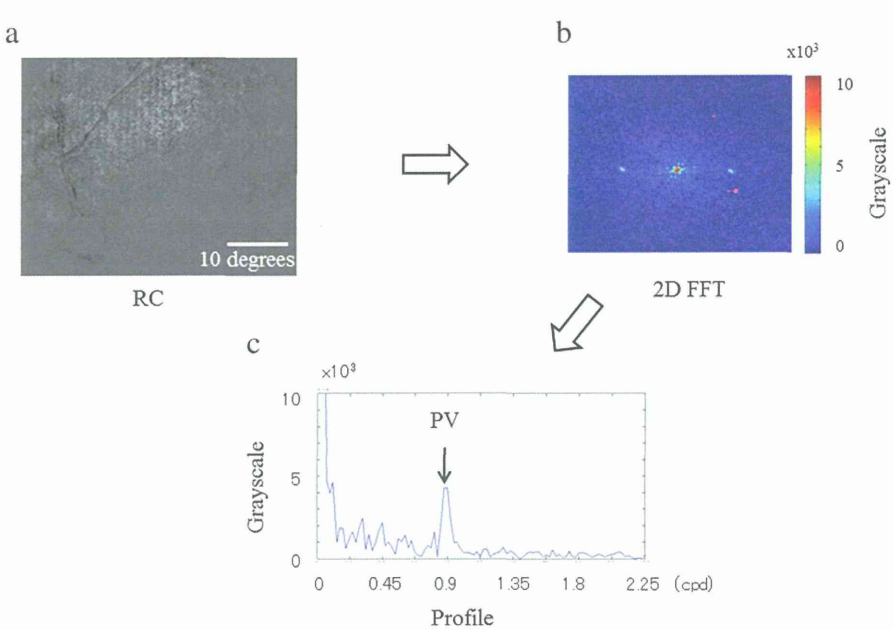

Fig. 2. Method to detect the peak value from the two dimensional FFT image. a. The reflectance changes (RC) in the retina in response to grating stimuli of 0.86 cpd. b. A 2-dimensional (2D) fast Fourier transform (FFT) of the reflectance changes. c. Profile of 2D FFT. The peak value (PV) is seen at a spatial frequency of 0.86 cpd.

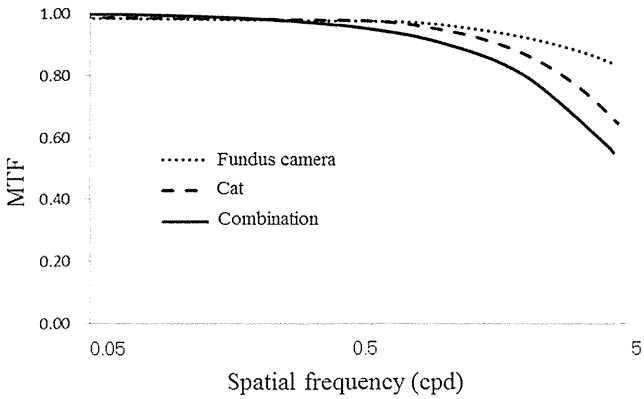

Fig. 3. Modulation Transfer Functions (MTFs) calculated from the wavefront aberration of the eyes of cats and that of fundus camera and combination of those of MTF.

Because the signals elicited by gratings >1 cpd were difficult to distinguish by the reflectance change images, we used the FFT method to analyze the spatial tuning of the reflectance changes.

We also measured the optical properties of cat eyes using a custom-built wavefront sensor with a 2 mm pupil. The MTF decreased monotonically from low to higher spatial frequencies, and the MTF was more than 0.8 at 3.46 cpd (Fig. 3). Bonds (1974) measured the MTF of cat eyes from the line spread function with a 2 mm pupil and the value decreased monotonically and was 0.7 at a spatial frequency of 3 cpd. Thus, our findings are consistent with those of Bonds.

Light absorbance was predominant in the range of 730–770 nm which is due to the greater absorption by deoxy-hemoglobin (Hb) than by oxy-hemoglobin (HbO_2) whose absorption is more in the range of 780–820 nm while that of HbO_2 is higher in the range of 830–880 nm (Hirohara et al., 2007). In an earlier study, we found that after electrical stimulation of the retina, the time course of RC was different for veins and arteries (Mihashi et al., 2011). The time course of the changes in the peak value was almost identical for the different wavelengths of light (Fig. 5). These results suggest that the peak value is not related to the oxygen saturation of the blood.

The amplitude of the peak value was lower at longer wavelengths (Fig. 5) which would suggest that the mechanism underlining the RCs had a higher sensitivity at longer wavelengths.

The peak value was highest at the lowest spatial frequency (0.05 cpd) and decreased steeply with an increase of the spatial frequency and was almost absent at 3.46 cpd (Figs. 6 and 7). The different spatial response patterns between the peak value curve and the MTF curve suggest that the peak value does not simply reflect the activity of the photoreceptors.

Schallek et al. (2009a) used an intravitreal injection of tetrodotoxin in cats to study the origin of the intrinsic signals of the retina after light stimulation. They concluded that the signals originated mainly from the outer layers of the retina. However, Tsunoda et al. (2009) reported that a slow component of the intrinsic signal elicited by a flash of light stimuli decreased in the peripheral retina after the injection of tetrodotoxin in macaque monkeys. They suggested that the retinal ganglion cells contributed to the retinal intrinsic signal.

Li et al. (2010) examined the intrinsic signal elicited by a 500 ms visible light flash on frog retinal slices. A fast response

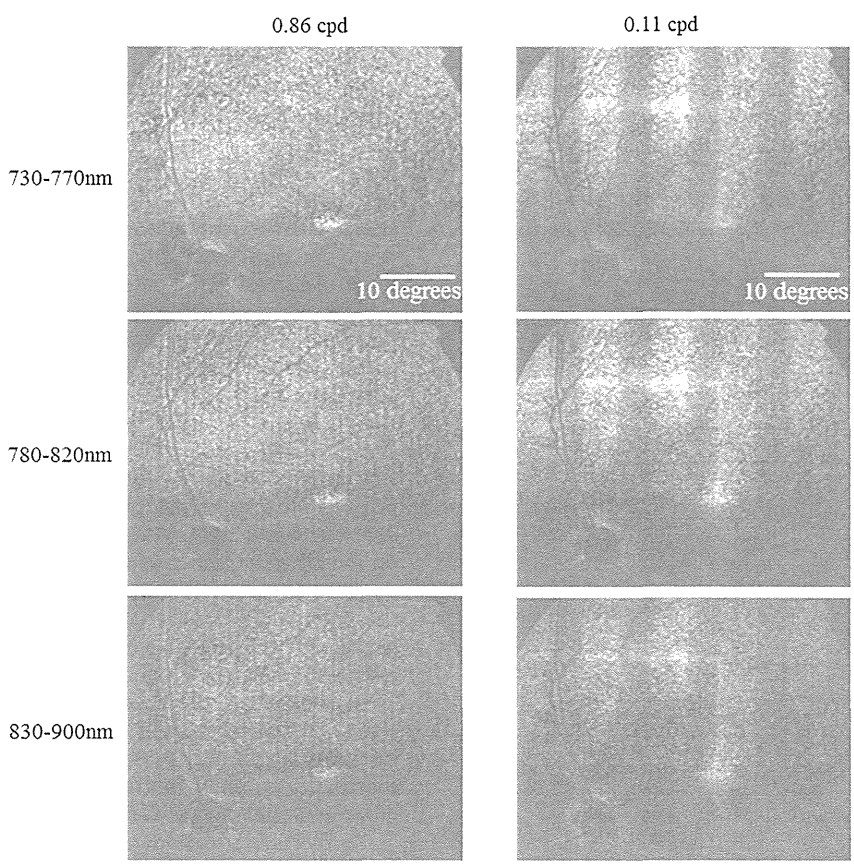

Fig. 4. Typical images of the reflectance change in response to grating stimuli of 0.11 and 0.86 cpd with different ranges of wavelength.

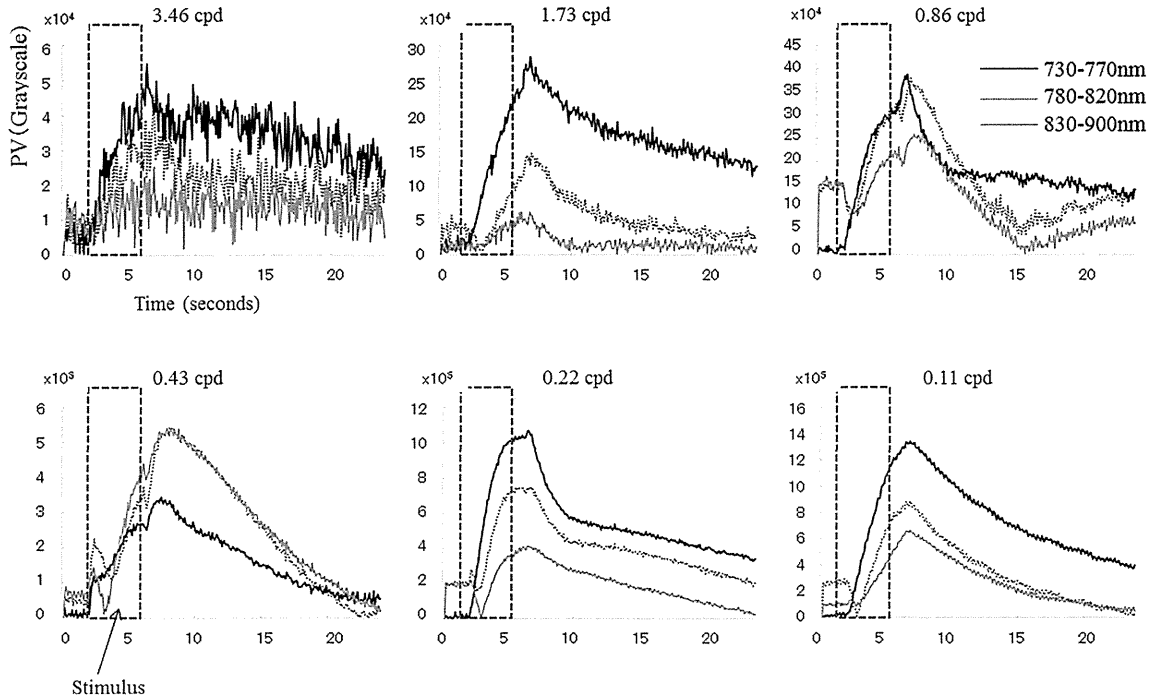

Fig. 5. *Time course of peak values for different wavelengths and different spatial frequencies in cat 4.*

was observed at photoreceptor layer and reached its peaks within 100 ms and a late response was observed in inner plexiformlayer (IPL) and reached its peaks at >1.5 s after the onset of light stimulus. The intrinsic signal in the photoreceptor layer was confined to the area of light stimulation, while that in the inner retinal layers spread from the stimulus site into a relatively large area. Because, the late responses in IPL of frog retinal slice was not due to the direct nerve activity or vascular changes, a possibility exists that they may reflect light scattering changes at the nerve terminal.

The time course of the intrinsic signal in our experiment was similar to that in the IPL of frogs (Li et al., 2010) (Fig. 5). If the intrinsic signals in our experiments are related to the signals in the IPL, the spatial pattern of intrinsic signal should be blurred and would not be resolved at high spatial frequencies as was found in our experiments (Fig. 6).

Ohzawa and Freeman (1985) studied the pattern ERGs elicited by square wave, phase reversal stimuli and reported that the amplitude decreased monotonically with an increase of spatial frequency from 0.07 cpd. The amplitude was almost unrecordable at 3 cpd. The grating stimuli in our study were the on-type of stimuli in which gratings appeared form the black background periodically. Therefore, the linear component of the intrinsic signal is evaluated in response to the grating stimuli, which is different from the non-linear component which is evaluated by phase-reversal stimuli in the pattern ERGs.

The response pattern in relation to the spatial frequency of the pattern ERGs is quite similar to that of our study (Fig. 7). The pattern ERGs represent the activity of retinal ganglion cells (Shorstein et al., 1999), so a possibility exists that the intrinsic signals elicited by gratings are related to the activity of retinal ganglion cells.

The implicit times, time from the onset of stimulation to the peak of intrinsic signal, was about 4 s and did not change with different wavelengths (Table 1). The implicit times of pattern ERGs, on the other hand, are reported to vary with different spatial frequencies (Shorstein et al., 1999). This discrepancy may be because the pattern ERGs reflect the neuronal activity directly, while the retinal intrinsic signal represents retinal structural or metabolic changes secondary to neural activation.

In conclusion, the reflectance pattern of the retinal intrinsic signal elicited by gratings of different spatial frequencies was different from that of the MTF. This suggests that the intrinsic signal represents not only the response of the photoreceptors but also other neuronal or vascular changes in the retina.

Further investigations with pharmacological agents are needed to determine the exact mechanism that determines the peak values.

Table 1
a) The times for peak value of PV. b) The normalized peak values of PV.

a)				
Frequency (cpd)	Average (seconds)			*P*-value
	730–770 nm	770–830 nm	830–900 nm	
3.46	6.56 ± 0.56	6.15 ± 0.48	6.25 ± 0.75	0.161
1.73	6.70 ± 0.67	6.45 ± 0.66	6.43 ± 0.35	0.477
0.86	6.36 ± 0.41	6.43 ± 0.41	6.31 ± 0.69	0.683
0.43	6.14 ± 0.32	6.25 ± 0.23	6.73 ± 0.74	0.009
0.22	6.24 ± 0.19	6.25 ± 0.12	6.34 ± 0.18	0.208
0.11	6.23 ± 0.21	6.23 ± 0.22	6.36 ± 0.20	0.035
0.05	6.22 ± 0.57	6.19 ± 0.68	6.42 ± 0.66	0.347
b)				
Frequency (cpd)	Average ($\times 10^{-4}$)			*P*-value
	730–770 nm	770–830 nm	830–900 nm	
3.46	0.25 ± 0.06	0.27 ± 0.11	0.16 ± 0.08	0.001
1.73	1.15 ± 0.53	0.79 ± 0.27	0.48 ± 0.30	<0.001
0.86	2.43 ± 0.90	1.87 ± 0.73	1.30 ± 0.50	<0.001
0.43	4.01 ± 2.52	2.82 ± 1.33	1.86 ± 1.07	<0.001
0.22	6.94 ± 2.32	4.61 ± 1.74	2.60 ± 0.92	<0.001
0.11	10.13 ± 3.99	6.65 ± 2.71	3.56 ± 1.38	<0.001
0.05	10.73 ± 3.95	6.70 ± 2.17	3.25 ± 1.13	0.001

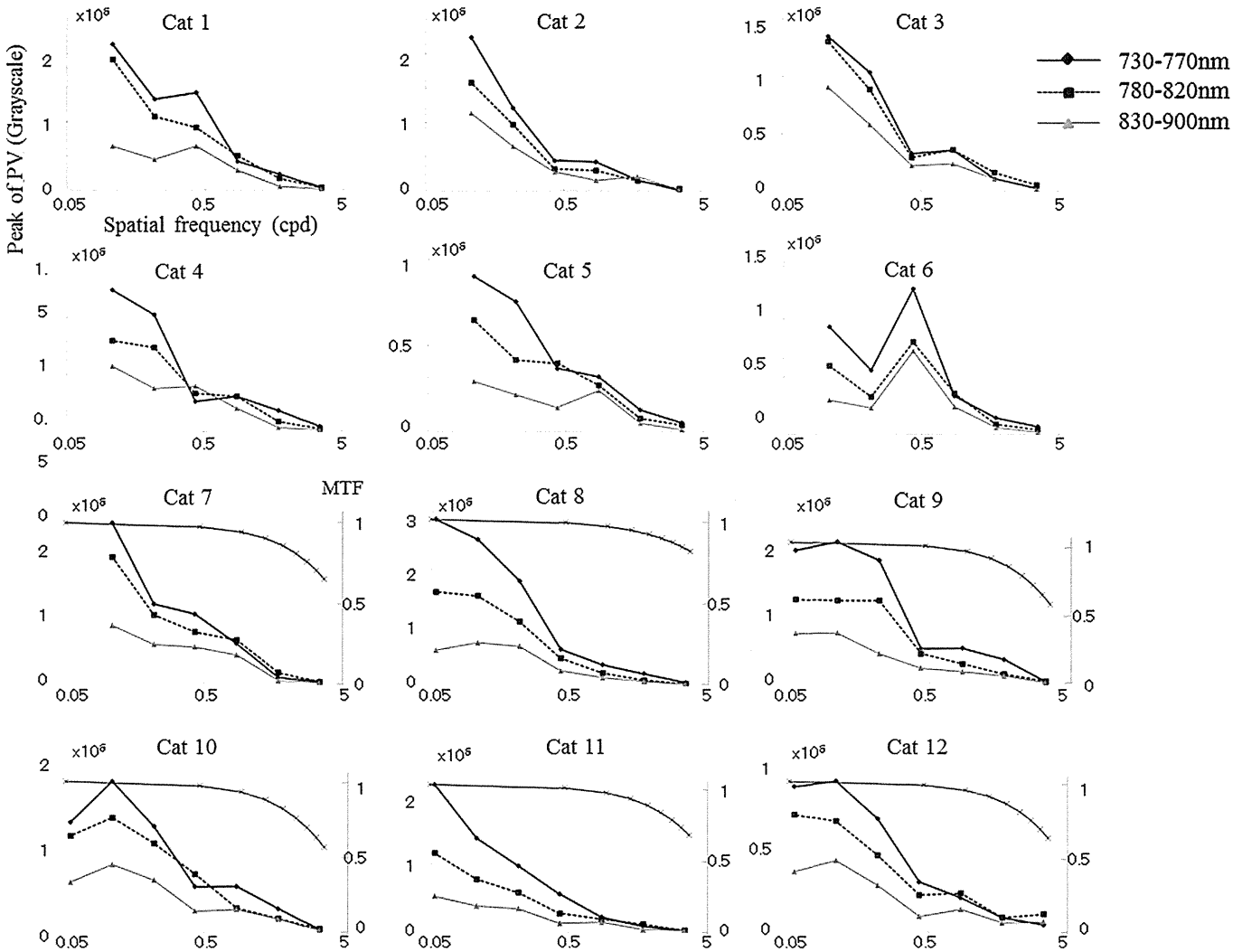

Fig. 6. The peak value of the relationship to the spatial frequency in each cat.

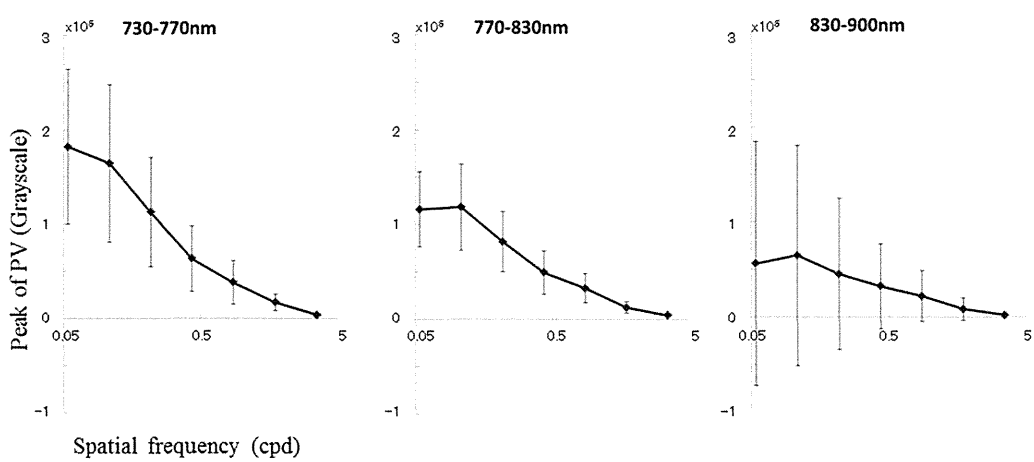

Fig. 7. The average of the maximum of the peak value showing the time course in relation to the spatial frequencies for different wavelengths ($n = 12$). Bars represent the standard deviation.

Financial support

This study was supported by Health Sciences Research Grants (H24-medical device – 001) from the Ministry of Health, Labor and Welfare, Japan and by Strategic Research Program for Brain Sciences from the Ministry of Education, Culture, Sports, Science and Technology, Japan.

Acknowledgment

The authors thank Dr. Hajime Sawai for the helpful discussion.

References

Bonds, A.B., 1974. Optical quality of the living cat eye. The Journal of Physiology 243, 777–795.

Cook, P.B., McReynolds, J.S., 1998. Lateral inhibition in the inner retina is important for spatial tuning of ganglion cells. Nature Neuroscience 1, 714–719.

Crittin, M., Riva, C.E., 2004. Functional imaging of the human papilla and peripapillary region based on flicker-induced reflectance changes. Neuroscience Letters 360, 141–144.

Diedrich, E., Schaeffel, F., 2009. Spatial resolution, contrast sensitivity, and sensitivity to defocus of chicken retinal ganglion cells in vitro. Visual Neuroscience 26, 467–476.

Enroth-Cugell, C., Robson, J.G., 1966. The contrast sensitivity of retinal ganglion cells of the cat. The Journal of Physiology 187, 517–552.

Fujikado, T., 1994. The effect of dopamine on the response to pattern stimulation – study of the chick ERG. Japanese Journal of Ophthalmology 38, 368–374.

Hanazono, G., Tsunoda, K., Kazato, Y., Tsubota, K., Tanifuji, M., 2008. Evaluating neural activity of retinal ganglion cells by flash-evoked intrinsic signal imaging in macaque retina. Investigative Ophthalmology & Visual Science 49, 4655–4663.

Hirohara, Y., Okawa, Y., Mihashi, T., Yamaguchi, T., Nakazawa, N., Tsuruga, Y., Aoki, H., Maeda, N., Uchida, I., Fujikado, T., 2007. Validity of retinal oxygen saturation analysis: hyperspectral imaging in visible wavelength with fundus camera and liquid crystal wavelength tunable filter. Optical Review 14, 151–158.

Inomata, K., Tsunoda, K., Hanazono, G., Kazato, Y., Shinoda, K., Yuzawa, M., Tanifuji, M., Miyake, Y., 2008. Distribution of retinal responses evoked by transscleral electrical stimulation detected by intrinsic signal imaging in macaque monkeys. Investigative Ophthalmology & Visual Science 49, 2193–2200.

Li, Y.C., Strang, C., Amthor, F.R., Liu, L., Li, Y.G., Zhang, Q.X., Keyser, K., Yao, X.C., 2010. Parallel optical monitoring of visual signal propagation from the photoreceptors to the inner retina layers. Optics Letters 35, 1810–1812.

Mihashi, T., Okawa, Y., Miyoshi, T., Kitaguchi, Y., Hirohara, Y., Fujikado, T., 2011. Comparing retinal reflectance changes elicited by transcorneal electrical retinal stimulation with those of optic chiasma stimulation in cats. Japanese Journal of Ophthalmology 55, 49–56.

Ohzawa, I., Freeman, R.D., 1985. Pattern evoked potentials from the cat's retina. Journal of Neurophysiology 54, 691–700.

Okawa, Y., Fujikado, T., Miyoshi, T., Sawai, H., Kusaka, S., Mihashi, T., Hirohara, Y., Tano, Y., 2007. Optical imaging to evaluate retinal activation by electrical currents using suprachoroidal-transretinal stimulation. Investigative Ophthalmology & Visual Science 48, 4777–4784.

Schallek, J., Kardon, R., Kwon, Y., Abramoff, M., Soliz, P., Ts'o, D., 2009a. Stimulus-evoked intrinsic optical signals in the retina: pharmacologic dissection reveals outer retinal origins. Investigative Ophthalmology & Visual Science 50, 4873–4880.

Schallek, J., Li, H., Kardon, R., Kwon, Y., Abramoff, M., Soliz, P., Ts'o, D., 2009b. Stimulus-evoked intrinsic optical signals in the retina: spatial and temporal characteristics. Investigative Ophthalmology & Visual Science 50, 4865–4872.

Shorstein, N.H., Dawson, W.W., Sherwood, M.B., 1999. Mid-peripheral pattern electrical retinal responses in normals, glaucoma suspects, and glaucoma patients. The British Journal of Ophthalmology 83, 15–23.

Sieving, P.A., Steinberg, R.H., 1987. Proximal retinal contribution to the intraretinal 8-Hz pattern ERG of cat. Journal of Neurophysiology 57, 104–120.

Smith 3rd, E.L., Kee, C.S., Ramamirtham, R., Qiao-Grider, Y., Hung, L.F., 2005. Peripheral vision can influence eye growth and refractive development in infant monkeys. Investigative Ophthalmology & Visual Science 46, 3965–3972.

Tsunoda, K., Hanazono, G., Inomata, K., Kazato, Y., Suzuki, W., Tanifuji, M., 2009. Origins of retinal intrinsic signals: a series of experiments on retinas of macaque monkeys. Japanese Journal of Ophthalmology 53, 297–314.

OPEN ACCESS Freely available online

PLOS ONE

Characteristics of Retinal Reflectance Changes Induced by Transcorneal Electrical Stimulation in Cat Eyes

Takeshi Morimoto[1]*, Hiroyuki Kanda[1], Tomomitsu Miyoshi[2], Yoko Hirohara[3], Toshifumi Mihashi[4], Yoshiyuki Kitaguchi[1], Kohji Nishida[5], Takashi Fujikado[1]

1 Department of Applied Visual Science, Osaka University Graduate School of Medicine, Suita, Osaka, Japan, **2** Department of Integrative Physiology, Osaka University Graduate School of Medicine, Suita, Osaka, Japan, **3** Research Institute, Topcon Corporation, Itabashi-ku, Tokyo, Japan, **4** Innovative Research Initiatives, Tokyo Institute of Technology, Yokohama, Kanagawa, Japan, **5** Department of Ophthalmology, Osaka University Graduate School of Medicine, Suita, Osaka, Japan

Abstract

Transcorneal electrical stimulation (TES) activates retinal neurons leading to visual sensations. How the retinal cells are activated by TES has not been definitively determined. Investigating the reflectance changes of the retina is an established technique and has been used to determine the mechanism of retinal activation. The purpose of this study was to evaluate the reflectance changes elicited by TES in cat eyes. Eight eyes of Eight cats were studied under general anesthesia. Biphasic electrical pulses were delivered transcornealy. The fundus images observed with near-infrared light (800–880 nm) were recorded every 25 ms for 26 s. To improve the signal-to-noise ratio, the images of 10 consecutive recordings were averaged. Two-dimensional topographic maps of the reflective changes were constructed by subtracting images before from those after the TES. The effects of different stimulus parameters, e.g., current intensity, pulse duration, frequency, and stimulus duration, on the reflective changes were studied. Our results showed that after TES, the reflective changes appeared on the retinal vessels and optic disc. The intensity of reflectance changes increased as the current intensity, pulse duration, and stimulation duration increased ($P<0.05$ for all). The maximum intensity of the reflective change was obtained when the stimulus frequency was 20 Hz. The time course of the reflectance changes was also altered by the stimulation parameters. The response started earlier and returned to the baseline later with higher current intensities, longer pulse durations, but the time of the peak of the response was not changed. These results showed that the reflective changes were due to the activation of retinal neurons by TES and might involve the vascular changes induced by an activation of the retinal neurons.

Citation: Morimoto T, Kanda H, Miyoshi T, Hirohara Y, Mihashi T, et al. (2014) Characteristics of Retinal Reflectance Changes Induced by Transcorneal Electrical Stimulation in Cat Eyes. PLoS ONE 9(3): e92186. doi:10.1371/journal.pone.0092186

Editor: Friedemann Paul, Charité University Medicine Berlin, Germany

Received August 20, 2013; **Accepted** February 20, 2014; **Published** March 20, 2014

Funding: This research was supported by Charitable Trust Fund for Ophthalmic Research in Commemoration of Santen Pharmaceutical's Founder. The funder had no role in study design, data collection and analysis, decision to publish, or preparation of the manuscript.

Competing Interests: The authors have the following interests: This research was supported by Charitable Trust Fund for Ophthalmic Research in Commemoration of Santen Pharmaceutical's Founder. Yoko Hirohara is the employee of Topcon Corporation. Toshifumi Mihashi was the employee of Topcon Corporation until 2012. There are no patents, products in development or marketed products to declare. This does not alter the authors' adherence to all the PLOS ONE policies on sharing data and materials, as detailed online in the guide for authors.

* E-mail: takeshi.morimoto@ophthal.med.osaka-u.ac.jp

Introduction

Transcorneal electrical stimulation (TES) activates retinal neurons and evokes electrical potential changes in the visual cortex. These changes lead to visual sensations in humans [1–3]. TES is used clinically for the treatment of optic neuropathy and retinal diseases [4–7] and for the determination of residual retinal function in patients with advanced retinitis pigmentosa (RP) [8–11]. Although electrophysiological studies have been performed to try to determine how TES activates retinal neurons [12,13], it has not been determined definitively because it is difficult to record electrically evoked retinal responses because of the artifacts induced by the electrical stimuli [14].

In situ optical imaging of the intrinsic signals is a well-established method of studying brain physiology and mapping the functional architecture of the cerebral cortex [15–17]. The intrinsic signals are represented by the optical reflectance changes associated with the activity of neural tissues [15–17]. The reflectance changes of neural tissues have been attributed to the physiological oximetric changes [16,17], blood flow changes [16,18], and light-scattering changes [19].

Optical imaging of the intrinsic signals of the retina has also been extensively studied [20–31], and it has become an established technique to investigate how the retina is activated by electrical currents [22,24,27,30]. However, the details of how the electrical stimuli affect the reflectance changes have not been determined.

Thus, the purpose of this study was to evaluate the retinal reflectance changes elicited by different stimulation parameters of the TES in cat eyes. We shall show that the reflectance changes appeared on the blood vessels and the optic disc, and the intensity of the reflectance changes was dependent on the parameters of the electrical stimuli. These reflective changes were due to the activation of retinal neurons by TES and might involve the vascular changes induced by an activation of the retinal neurons.

Materials and Methods

Ethics Statement

All experiments were performed in accordance with the ARVO Statement for the Use of Animals in Ophthalmic and Vison Research, and all procedures were approved by the Animal

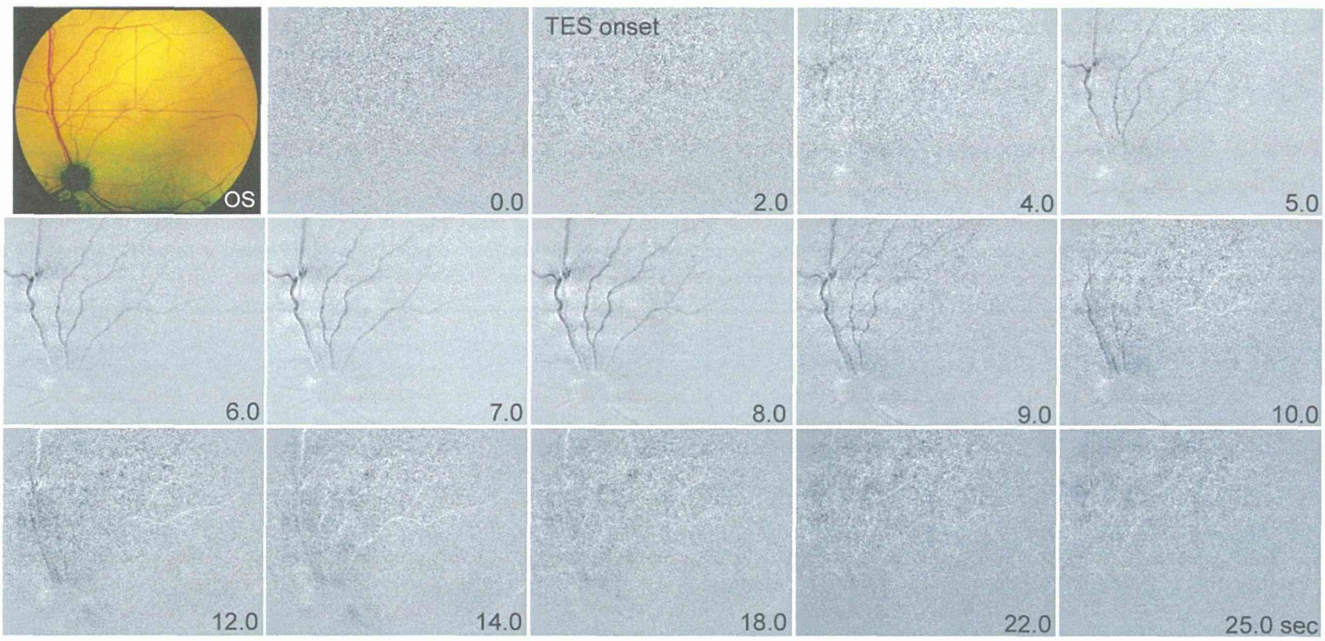

Figure 1. Images of the fundus of the eye of a cat showing reflectance changes in response to transcorneal electrical stimulation (TES). The reflectance changes appeared on the optic disc (OD) and over the retinal blood vessels after the TES. The reflectance changes began about 2.0 s after the onset of stimulation (4.0 s after the onset of recording), and the intensity of the reflectance change increased for 7.0 s after the onset of the recording. It then gradually decreased for 12.0 s. The top left is a fundus photograph of the left eye.
doi:10.1371/journal.pone.0092186.g001

Research Committee of Osaka University graduate school of medicine.

All efforts were made to minimize suffering.

Animals and Preparation

Eight healthy adult cats between 7 months and 1-year-of-age of both sexes and weighing 2.5–3.0 kg were studied. These cats were raised in a breeding colony in the Institute of Laboratory Animals, Osaka University, Graduate School of Medicine. The cats were initially anesthetized with an intramuscular injection of ketamine HCl (25 mg/kg) followed by an intraperitoneal injection of atropine sulfate (0.1 mg/kg). The anesthesia and paralysis were maintained with a continuous intravenous infusion of sodium pentobarbital (1.0 mg/kg/hr), pancuronium bromide (0.2 mg/kg/hr), glucose (0.1 g/kg/hr) in Ringer's solution at a rate of 5 ml/hr. The cats were artificially ventilated with a mixture of N_2O/O_2 (1:1), and the end-tidal CO_2 concentration was kept at 3.5 to 5.0% by altering the frequency and tidal volume of the ventilation. The intratracheal pressure and electrocardiogram were also monitored. The body temperature was maintained at 38°C with a heating pad.

Only the left eyes of the cats were studied due to equipment and space limitations. The pupil was dilated with a solution of 0.5% tropicamide and 0.5% phenylephrine hydrochloride, and 1% atropine. A closed ring shaped eyebar made of stainless steel was used to stimulate the eye. The ring (diameter, 16.5 mm) of the eyebar was sutured to the limbus of cornea, and the end of the bar of the ring was attached to the stereotaxic headholder to minimize eye movements. To protect the corneal surface, a hard contact lens (polymethylmethacrylate; base curve, 8.50 mm; diameter, 13.5 mm; power, +1.5 diopters) was placed on the cornea. The corneas were kept moist with drops of a 0.9% NaCl solution during the experiment.

Optical Imaging of Reflectance Changes of Retina

The ocular fundus was viewed with a fundus camera (TRC-50LX, Topcon, Tokyo, Japan) equipped with a digital CCD camera (C8484, Hamamatsu Photonics, Hamamatsu, Japan) [22,31]. The resolution of the camera was 1280×1024 pixels, but the use of the binning mode of the camera to obtain maximum light sensitivity reduced the resolution to 320×256 pixels (12-bit gray scale). A 12-bit digitizer was used, and 4096 grayscale values (GSVs) were obtained for each pixel. The exposure time of the CCD imaging was 20 ms.

A halogen lamp was used to illuminate the posterior fundus, and a band-pass filter was inserted into the optical path to limit the wavelength of the fundus monitoring light to 800–880 nm [22,31]. The power of the monitor light was 250 nW, which was much lower than the safe exposure limit of the American National Standards Institute.

Fundus images were obtained every 25 ms for 26 s. The images were recorded 2 s before, 4 s during, and 20 s after the electrical stimulation. To improve the signal-to-noise ratio, ten images of ten consecutive measurements were averaged [22,31]. The interval between sessions was 1 min. A two-dimensional image of the reflectance changes was obtained by subtracting the images recorded before the stimulation from those recorded after the stimulation. A stabilized power supply (PS-150UE-DC, Hayashi Watch Works, Tateyama, Japan) was used to reduce background fluctuations of the illuminating light. All experiments were performed in a dark room after 30 min of dark-adaptation.

Transcorneal Electrical Stimulation

The left eyes were stimulated transcornealy by the sutured stainless eyebar shaped electrode at the sclerocorneal limbus as one of the electrodes. The return electrode was placed under the skin of the head. The TES consisted of rectangular anodic first (cornea positive) biphasic current pulses obtained from an

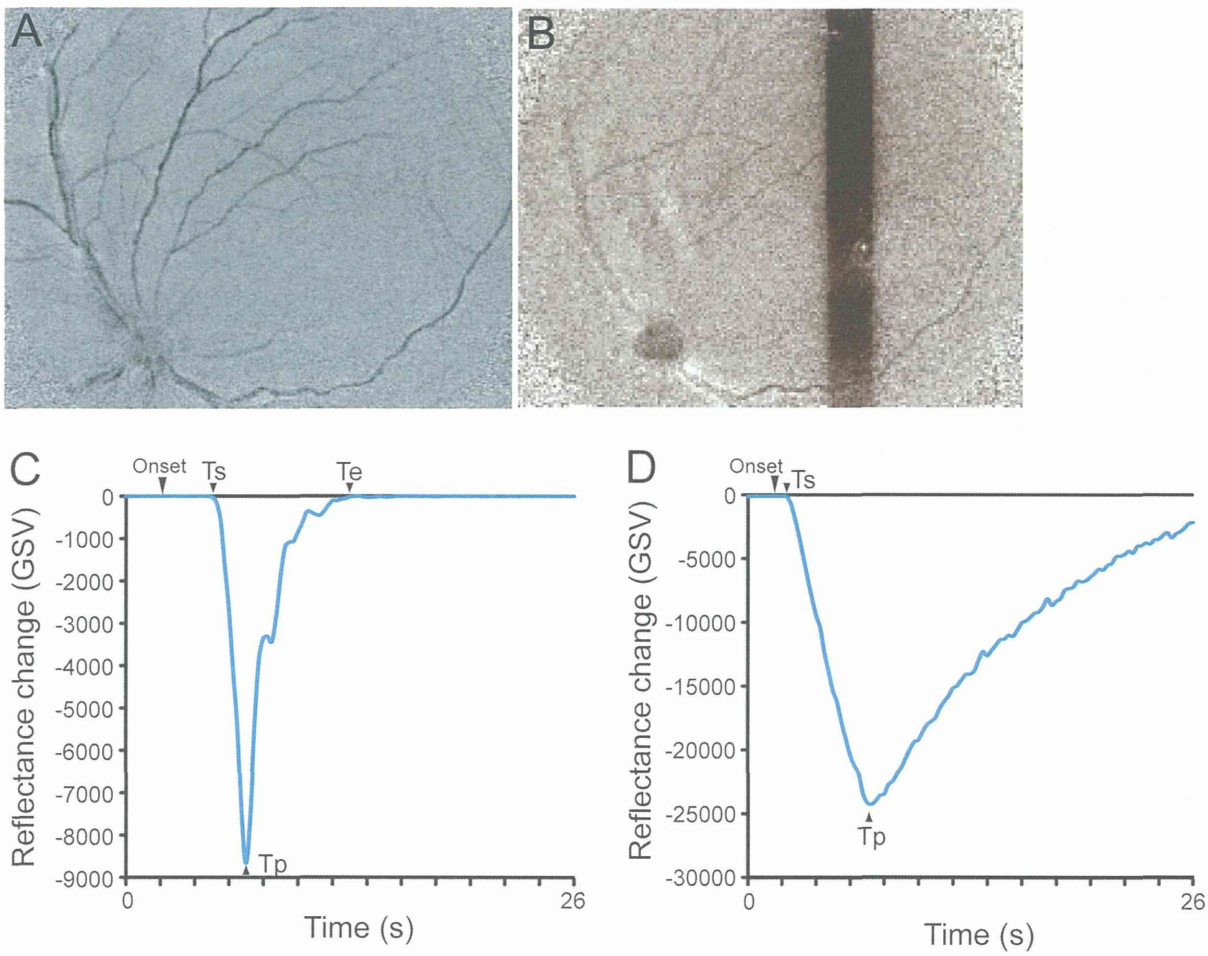

Figure 2. Images of reflectance changes elicited by TES (A) and by photic stimulation (B). The reflectance changes on the OD and over the retinal blood vessels decreased after TES (A), while reflectance changes evoked by light stimulation appeared at the light-stimulated retinal area, the retinal vessels, and OD (B). Plot of the time course of the reflectance changes evoked by TES (C) and light stimulation (D). The latency of the light stimulated retina (D) was shorter than that after TES (C), but the implicit time of the response was same. The time to return to the baseline in the light stimulated retina (D) was significantly later than that after TES (C).
doi:10.1371/journal.pone.0092186.g002

electrical stimulation system (Stimulator: SEN-7203, Nihon Kohden, Tokyo, Japan; Isolator: BSI-950, Dagan, Minneapolis, MN, USA). To examine the relationship between the stimulus parameters and the intensity of the reflectance changes, the stimulus parameters were changed: current intensities of 0.1,0.5, 1.0, and 2.0 mA of 5 ms/phase at 20 Hz at 20 pulses; pulse durations of 0.5,1.0, 2.0, 3.0, 5.0, and 10.0 ms/phase with constant current intensity at 20 Hz at 20 pulses; frequencies of 5, 10, 20, 30, and 50 Hz at constant current intensity of 5 ms/phase at 20 pulses; and stimulation duration of 0.5, 1, and 4 sec of 5 ms/phase at 50 Hz.

Light Stimulation of Retina

The eye was stimulated with a 4° vertical bar at 8 Hz for 4 s. The bar was presented 6° temporal to the area centralis. The light power was 30 nW.

Electrophysiological Recordings from Optic Chiasma

The tips of a pair of stainless steel electrodes was placed in the optic chiasma (OX) stereotaxically to record the electrical potential changes evoked by electrical stimulation of the retina. This was done to record the potential changes in the axons of the retinal ganglion cells elicited by TES. The electrode was inserted from the cortical surface at 13–14 mm anterior to the ear bard and 1–2 mm ipsilateral to the midline. The depth of the electrode tip was 23–26 mm from the cortical surface. Light-evoked responses were recorded from each electrode to be certain that the electrodes were placed in the OX.

To record the electrically evoked potentials (EEPs) by TES, the signal was amplified 10,000 times and bandpass filtered between 300 Hz and 5 kHz with an AC amplifier (Model 1800; Microelectrode AC amplifier; A-M Systems, Inc., Carlsborg, WA) and a signal conditioner (LPF-202A; Warner Instruments, Hamden, CT). Amplified EEPs were fed to a signal processor (Power 1401; Cambridge Electronic Design, Cambridge, UK) and were analyzed with a sampling frequency of 50 kHz offline. Signals were also monitored on an oscilloscope and an audio speaker in real time.

The amplitudes, latencies, and implicit times of the EEPs evoked by TES was measured. The amplitude was measured between the first negative through (N1) to the first positive peak (P1). The P1 latencies were also measured.

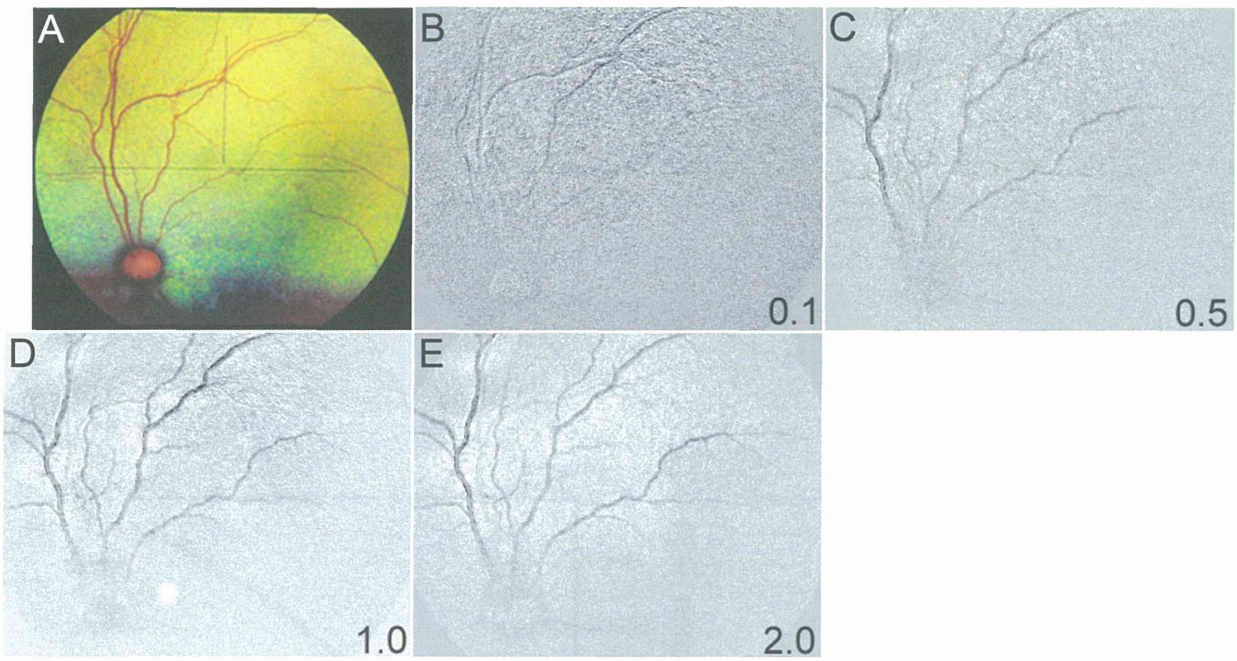
A
B
0.1
C
0.5
D
1.0
E
2.0

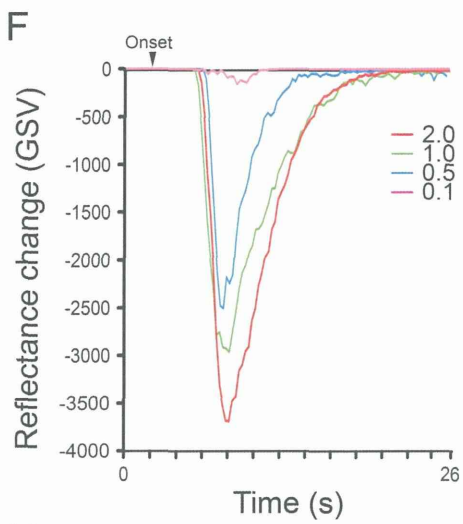
F
Onset
0
-500
-1000
-1500
-2000
-2500
-3000
-3500
-4000
Reflectance change (GSV)
2.0
1.0
0.5
0.1
0
26
Time (s)

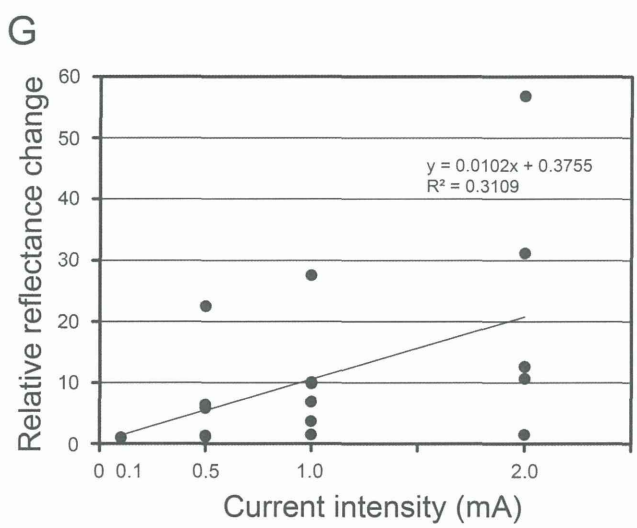
G
60
50
40
30
20
10
0
Relative reflectance change
y = 0.0102x + 0.3755
R² = 0.3109
0 0.1
0.5
1.0
2.0
Current intensity (mA)

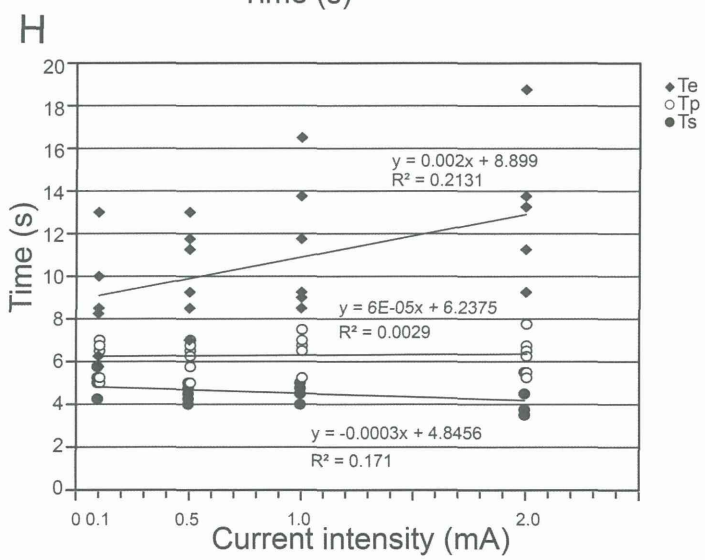
H
20
18
16
14
12
10
8
6
4
2
0
Time (s)
Te
Tp
Ts
y = 0.002x + 8.899
R² = 0.2131
y = 6E-05x + 6.2375
R² = 0.0029
y = -0.0003x + 4.8456
R² = 0.171
0 0.1
0.5
1.0
2.0
Current intensity (mA)

Figure 3. Effect of current intensity of TES on reflectance changes. Fundus photograph (A) and images of reflectance changes elicited by different current intensities (B–E). The GSVs of the reflectance changes (dark signal) decreased as the current intensity increased (F). The relative reflectance changes increase as the current intensities increase (G). The increase in the maximum relative reflectance changes as the current intensities increase was almost linear with stimulus currents up to 2.0 mA (G). There was a significant positive correlation between relative reflectance changes and current intensities ($r^2 = 0.311$, $P = 5 \times 10^{-4}$). A plot of the latency and current intensity is graphed in H. The latency decreases and time to return to baseline increases as the current intensity increases. The changes in the latency is significantly correlated with the current intensities ($r^2 = 0.1333$, $P = 0.045$). The reflectance changes are also significantly correlated with the current intensities ($r^2 = 0.213$, $P = 002$) (H).
doi:10.1371/journal.pone.0092186.g003

Data Analyses

To evaluate the intensity of the reflectance changes, the GSV of each spot of the retina within the fundus image was averaged. The averaged GSV of each spot after the onset of electrical stimulation was subtracted from that before the stimulation to obtain the change in the reflectance of the image. Each recording trial consisted of 300 video frames collected at 30 frames/s for a total recording time of 26 s. The GSVs of 15 video frames collected in 0.5 second were averaged for individual data points to determine the time course of the stimulation-induced reflectance changes. The data were used to plot the time courses of the reflectance changes.

The amplitude was calculated as poststimulus GSV/0.5-second pre-stimulus GSVs pixel by pixel as the relative reflectance changes. The relative reflectance changes were normalized for comparison among the cats, because the magnitude of reflectance changes varied for each cat.

We also analyzed the time course of reflectance changes to determine the latency as the start of the rise of the wave of the reflectance changes, the implicit time as the time to the peak of reflectance changes, the time when the reflectance change returned to the baseline.

Statistical Analyses

Data were analyzed with the JMP (ver. 9.0; SAS Institute Inc., NC) program. The data are expressed as the means ± standard error of the means. Regression analyses between the stimulus parameters and the intensity and latency of the reflectance changes or the amplitude and latency of the EEP at the OX was evaluated by JMP. Statistical significance was set at $P<0.05$.

Results

Characteristics of Retinal Reflectance Changes after TES

Two-dimensional maps of the reflectance changes after TES are shown in Figure 1. The reflectance changes appeared at the optic disc (OD) and retinal blood vessels about 2.0 s after the onset of stimulation (4.0 s after the onset of recording). The intensity of the reflectance changes continued to increase for 7.0 s and then gradually decreased for 12.0 s after the onset of the recordings.

Images of the reflectance changes after TES and light stimulation are compared in Figures 2A and 2B. The time course of the reflectance changes evoked by TES and light stimulation is shown in Figures 2C and 2D. There were some differences of images and time courses in the reflectance changes between TES and light stimulation. The GSV of the reflectance changes evoked by TES began to decrease about 5.0 s after the onset of recording and continued to decrease for 7.0 s (Fig. 2C). The GSV returned to the baseline at about 13.0 s (Fig. 2C).

The reflectance changes evoked by light stimulation appeared at the light-stimulated retinal area, the retinal vessels, and optic disc (OD) (Fig. 2B). The time course of the GSV of the reflectance changes evoked by light stimulation are plotted in Figure 2D. The GSV of the reflectance changes decreased just after the onset of light stimulation, and the latency of the reflectance changes (Ts) after the light stimulation was shorter than that after TES, but the implicit time of the peak of the reflectance changes (Tp) was the same. However, the time to return to the baseline (Te) in the light stimulated retina was significantly longer than that after TES (Figs. 2C, 2D).

Effect of Current Intensity of TES on Reflectance Changes

The effect of the strength of the electric current on the reflectance changes was determined for currents from 0 to 2.0 mA. The stimulus duration was 5.0 ms/phase, frequency was 20 Hz, and stimulation duration was 1.0 s. The GSV of the reflectance changes increased with an increase of electric current (Figs. 3A to 3F). The maximum relative reflectance changes increased almost linearly with an increase in the stimulus current up to 2.0 mA (Fig. 3G). Simple regression analysis showed that there was a significant positive correlation between relative reflectance changes and current intensities ($r^2 = 0.311$; $P = 0.005$; Fig.3G).

Three measurements of the time course of the reflectance changes are plotted in Figure 3H. It can be seen that the latency of the reflectance changes (Ts) and the time to return to the baseline (Te) were depended on the current intensity. There were significant correlations between these latencies and current intensities (Ts, $r^2 = 0.133$, $P = 0.045$; Te, $r^2 = 0.213$; $P = 0.023$; Fig. 3H).

Effect of Pulse Duration on Reflectance Changes

The effect of pulse duration on the reflectance changes was determined for pulse durations of 0.5 to 10.0 ms/phase. These experiments were done with a pulse frequency of 20 Hz; current intensity of 0.1 to 0.5 mA depending on the response; and stimulus duration time of 1.0 s. Our findings showed that the reflectance changes decreased with increasing pulse durations up to 10.0 ms/phase (Figs. 4A to 4G). The increase in the amplitudes of the relative reflectance changes depended on the pulse duration (Fig. 4H). Simple regression analysis showed that there was a significant positive correlation between the relative intensities of the reflectance changes and pulse durations ($r^2 = 0.432$; $P< 0.0001$).

The latency of a response (Ts) and time to the return to the baseline (Te) depended on the pulse duration (Figure 4I). The implicit times did not change significantly with pulse duration. There were significant correlations between the latency and time to return to baseline of the reflectance changes and pulse durations (Ts, $r^2 = 0.171$, $P = 0.009$; Te, $r^2 = 0.246$, $P = 0.001$; Fig. 4I).

Effect of Stimulation Duration on Reflectance Changes

The effect of stimulation duration on the reflectance changes was determined for stimulus durations of 0.4, 1.0, and 4.0 s. For these experiments, the pulse frequency was 50 Hz, current intensity was 0.1 to 0.5 mA depending on the response, and the pulse duration was 5 ms/phase. The relationship between the reflectance changes and the stimulation time showed that the reflectance changes also decreased almost linearly with the stimulation durations up to 4.0 s (Figs. 5A to 5E). The amplitudes of the relative reflectance changes increased and was depended on

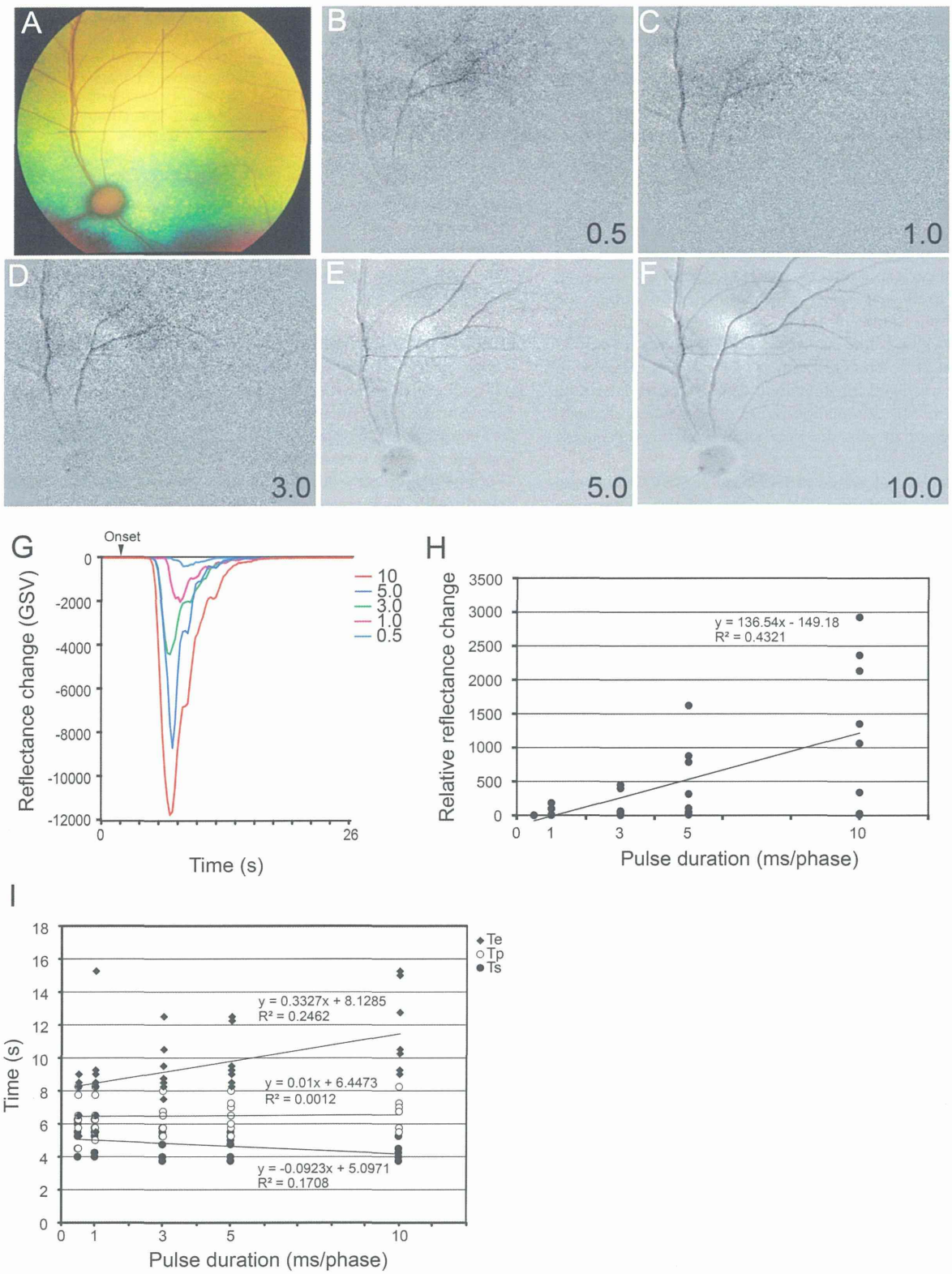

Figure 4. Effect of stimulus pulse duration on reflectance changes. Fundus photograph (A) and images of reflectance changes elicited by different pulse durations (B–F). The GSV of the reflectance changes (dark signal) decreases as the pulse duration increases (G). The relative reflectance changes increases as the pulse durations increase (H). The relative reflectance changes increases almost linearly with an increase of the pulse duration from 0.5 to 10.0 ms/phase (G). There is a significant positive correlation between the relative reflectance changes and pulse durations ($r^2 = 0.432$, $P < 1 \times 10^{-4}$). Plot of the relationship between the latency and pulse duration (H). The latency decreases as the pulse duration increases, but the time to return to the baseline increases as the pulse duration increases. The latency is significantly correlated with the pulse duration ($r^2 = 0.171$, $P = 0.009$), and the time to return to baseline was significantly correlated with the pulse durations ($r^2 = 0.246$, $P = 0.001$) (I).
doi:10.1371/journal.pone.0092186.g004

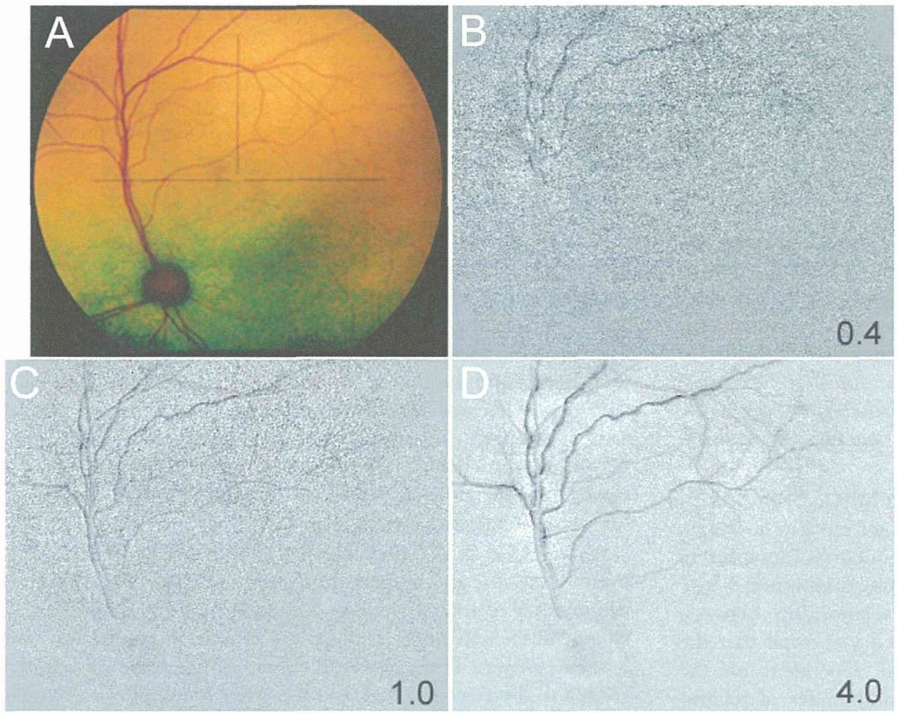
A
B
0.4
C
1.0
D
4.0

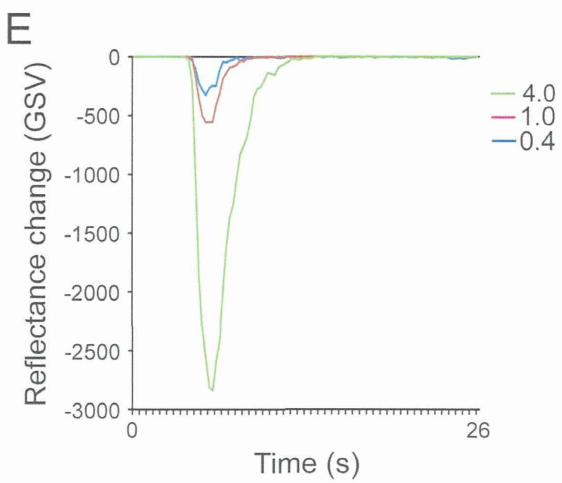
E
Reflectance change (GSV)
0
-500
-1000
-1500
-2000
-2500
-3000
0
26
Time (s)
4.0
1.0
0.4

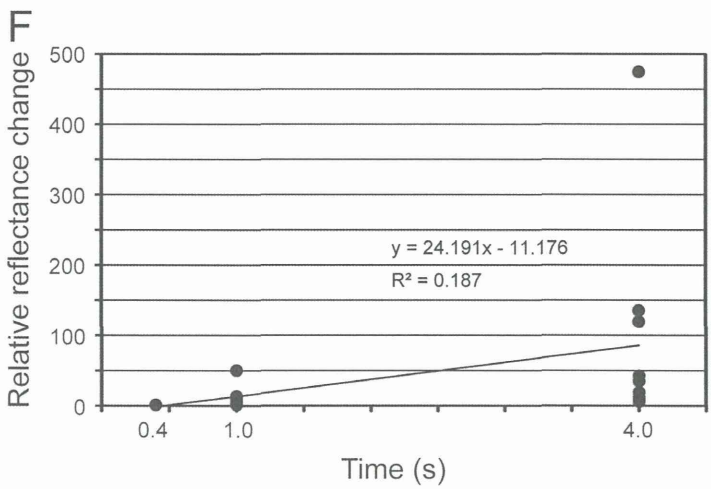
F
Relative reflectance change
500
400
300
200
100
0
y = 24.191x - 11.176
R² = 0.187
0.4
1.0
4.0
Time (s)

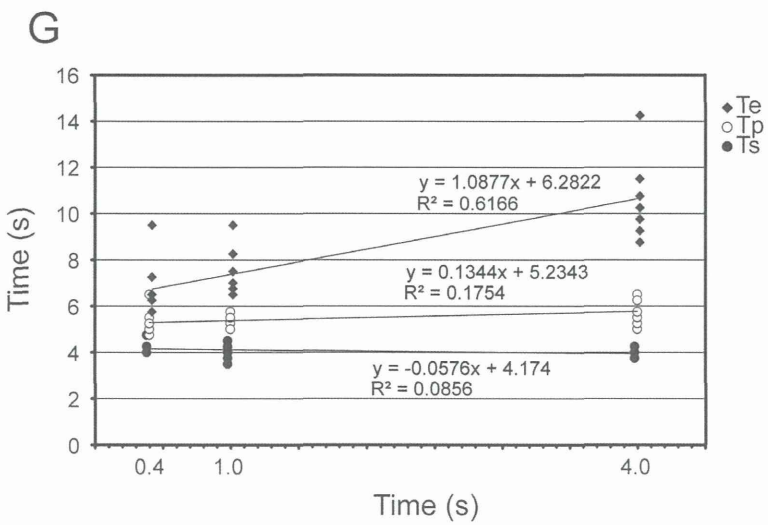
G
Time (s)
16
14
12
10
8
6
4
2
0
y = 1.0877x + 6.2822
R² = 0.6166
y = 0.1344x + 5.2343
R² = 0.1754
y = -0.0576x + 4.174
R² = 0.0856
0.4
1.0
4.0
Time (s)
Te
Tp
Ts

Figure 5. Effect of stimulation duration on reflectance changes. Fundus photograph (A) and images of the reflectance changes elicited by different stimulation durations (B–D). The GSV of reflectance changes (dark signal) decreases as the stimulation duration increases (E). Relative reflectance changes increases as the stimulation duration increases (F). There was an almost linear increase in the maximum relative reflectance changes and the stimulation duration from 0.4 to 4.0 s (F). There was a significant positive correlation between relative intensities of reflectance changes and the stimulation duration ($r^2 = 0.187$, $P = 0.017$). The relationship between latency and the stimulation time (G). The time to return to baseline increases as the stimulation duration increases. There was a significant correlation between the time to return to baseline and the stimulation duration ($r^2 = 0.086$, $P < 1 \times 10^{-4}$) (G).
doi:10.1371/journal.pone.0092186.g005

the stimulation duration (Fig. 5F). Simple regression analysis showed that there was a significant positive correlation between the relative intensities of the reflectance changes and stimulation duration ($r^2 = 0.187$, $P<0.017$). The time course of the reflectance changes are plotted in Figure 5G. The latency (Ts) and time to baseline (Te) increased as the stimulation duration increased. There was a significant positive correlation between the times (Ts, Te) and the stimulation duration (Ts, Te: $r^2 = 0.086$, $P<0.0001$).

Effect of Stimulus Frequency on Reflectance Changes

The effect of the stimulus frequency ranging from 5 to 50 Hz on the reflectance changes was determined with a current intensity of 0.1 to 0.5 mA depending on the response, pulse duration of 5 ms/phase, and pulse number of 20. The relationship between reflectance changes and the stimulus frequency showed that the GSV of the reflectance changes was also dependent on the stimulus frequency (Figs. 6A to 6G). The amplitudes of relative reflectance changes also changed depending on the frequency (Fig. 6H). Non-linear polynomial regression analysis showed that these data were best fitted by a non-linear equation (quadratic term; $P = 0.001$; Fig. 6H). The latencies of Ts, Tp, and Te are plotted in Figure 6I. There was no significant correlation between all of these measures and the stimulus frequencies.

Electrophysiological Recordings from Optic Chiasm after TES

We examined the relationship between the EEP amplitude recorded in the OX and the intensity of the stimulus currents. The EEP amplitude increased linearly with an increase of stimulus current (Figs. 7A, 7B), and linear regression analysis showed that there was a significant positive correlation between amplitudes of EEPs and the current intensities ($r^2 = 0.289$; $P = 0.001$). However, there was no significant correlation between the P1 latencies and the current intensities (Fig. 7C).

These results indicate that TES with the parameters used can activate retinal ganglion cells (RGCs) directly or indirectly and the degree of activation was significantly correlated with the intensity of electrical current. In addition, the EEP amplitudes were significantly correlated with the GSV of the reflectance changes of the retina ($P = 0.0011$; $r^2 = 0.4962$; Fig. 7D). This suggests that the reflectance changes represented the neuronal changes in the retina, i.e., the excitation of the RGCs.

Discussion

Our results showed that there were specific reflectance changes of the retina in response to the TES. The GSVs of the reflectance changes were significantly increased with higher current intensities, longer pulse durations, and longer stimulation durations. These findings indicate that the increase in the GSVs of the reflectance changes was due to the increase of the electrical flux. In addition, there was a frequency specificity with the maximum signals obtained with a stimulus frequency of 20 Hz, if the electrical flux was same at each frequency. Our findings are similar to those obtained from monkey eyes [24,28].

The relationship between the time course and stimulus parameters on the RCs has not been determined. We have determined the relationship between the time course and stimulus parameters on the RCs. The time course of the responses was also altered by the parameters of the TES. The latency of response (Ts) was shorter and the time to return to the baseline (Te) was longer with higher current intensities and longer pulse durations, but the time of the peak of the response (Tp) was not changed (Figs. 3H, 4I). When the current intensity and the pulse duration were the same, only the time to return to baseline (Te) was longer with longer stimulation durations (Fig. 5G).

An increase in the electrical flux by stronger currents, longer pulse durations, and longer stimulation durations should increase the number of retinal neurons activated by TES. Therefore, the latency of the reflectance changes are shorter and the return to the baseline longer. Thus, the time course of the response might be related to the electrical flux. On the other hand, the peak implicit time of the response (Tp) was not changed by the different parameters of the TES. This indicates that the reflectance changes occurred in response to a certain process, such as a neurological change to a vascular change.

What do Intrinsic Reflectance Changes Represent?

The reflectance changes evoked by TES appeared over the retinal vessels and optic disc, and these were different from those elicited by photic stimulation (Fig. 2s). Mihashi et al reported that the inhibition of the action potentials of retinal ganglion cells (RGCs) by tetrodotoxin (TTX) abolished the reflectance changes elicited by TES or by OX stimulation, but TTX did not induce significant changes in the retinal intrinsic signals elicited by photic stimulation [31]. These results suggest that the reflectance changes after either TES or OX stimulation were caused by the activation of the RGCs.

Although there was a significant correlation between the activity of RGCs and the reflectance changes, this does not directly indicate that they are due to the activation of the RGCs, because the latency of the response was much longer than that of action potentials of RGCs. The RCs represent the responses associated with hemodynamic changes in either the blood volume and flow or the oxygenated state of hemoglobin that is caused by the activity of the RGCs [32–35].

The existence of a fundamental relationship between neural activity, blood flow, and metabolism, called a neurovascular coupling, was suggested by Roy and Sherrington [32]. A neurovascular coupling in the optic nerve and retina was postulated by Riva et al [33]. The blood flow and local partial pressure of oxygen in the optic nerve have been shown to be modulated by intermittent light stimuli, and both were coupled to the activity of RGCs [34,35]. These findings indicate that the blood flow and metabolism in the retina and optic nerve can be modulated by local neural activity. Moreover TES has been shown to increase the chorioretinal blood flow in normal subjects with minimal effects on the systemic blood circulation and the intraocular pressure [36]. The increased retinal blood flow elicited by photic stimulation measured by laser Doppler flowmetry is

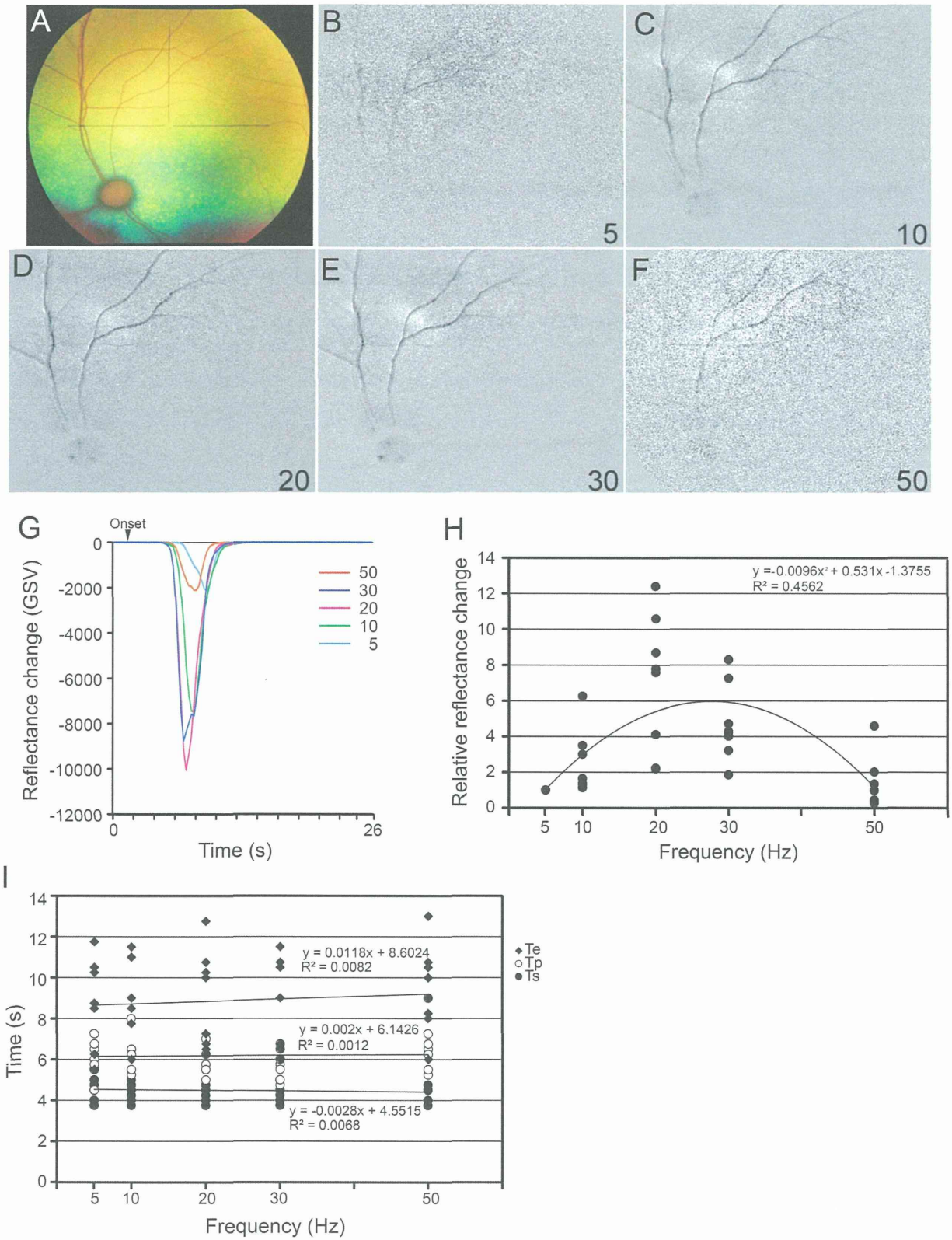

Figure 6. Effect of stimulus frequency on reflectance changes. Fundus photograph (A) and images of reflectance changes elicited by different stimulus frequencies (B–F). The GSV of the reflectance changes (dark signal) depended on the frequency (G), with the relative reflectance changes depended on the stimulus frequency (H). The maximum relative reflectance changes was best fit to the stimulus frequency by a non-linear curve (quadratic term; $P = 0.001$). The relationship between the latency and the frequencies (I). There was no significant correlation between latencies and stimulus frequencies.

doi:10.1371/journal.pone.0092186.g006

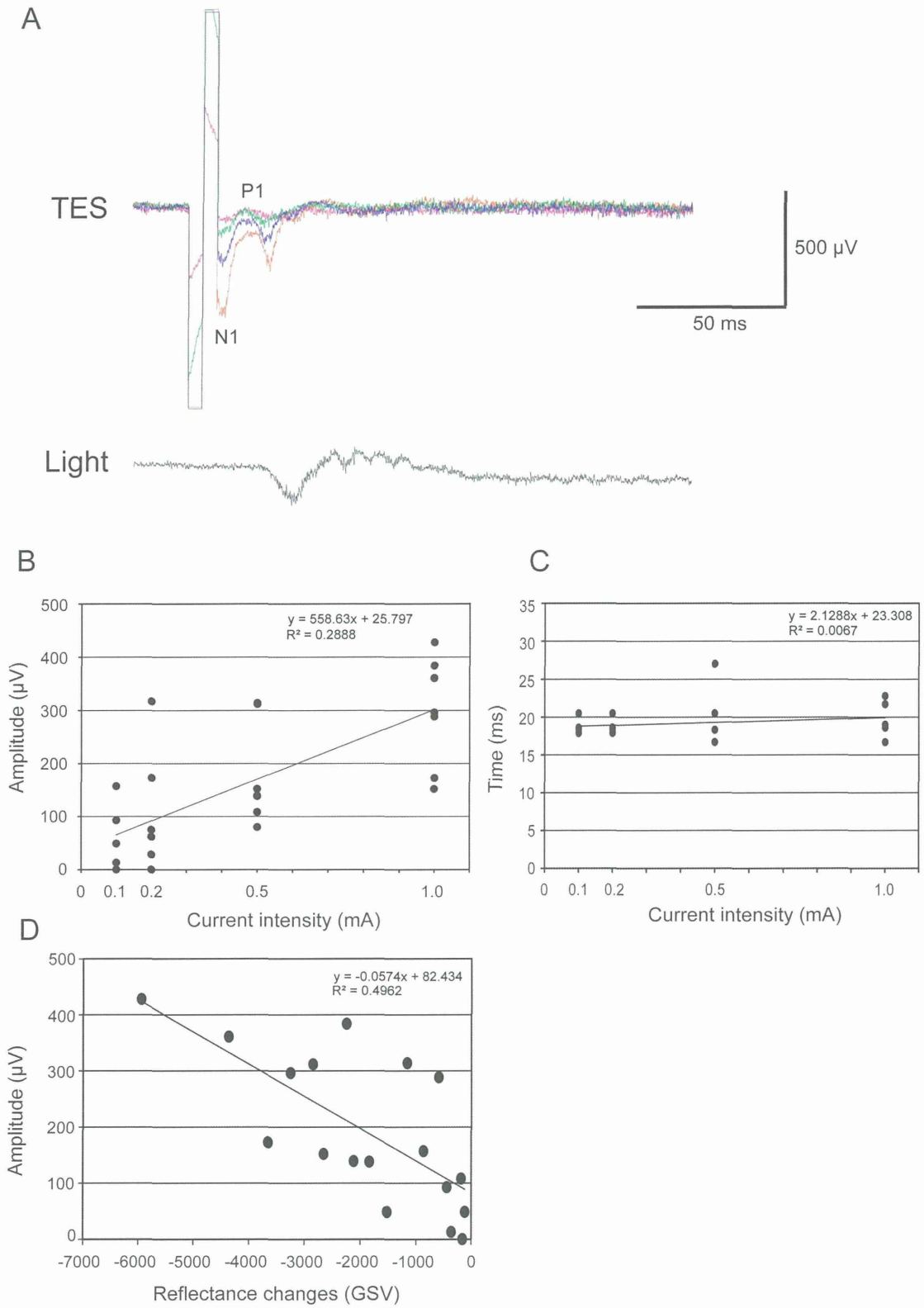

Figure 7. Electrophysiological recordings from the optic chiasm (OX) after TES. The electrically evoked potentials (EEPs, upper) and the light evoked potentials (VEPs, lower) are shown. Graph showing the relationship between the EEP amplitude and electric current (B) and the relationship between the peak latency (P1) and electric current (C). B. There was a significant positive correlation between amplitudes of EEPs and current intensities ($P = 0.0007$, $r^2 = 0.2888$). C. The relationship between the peak latency (P1) and electric current. There was no significant correlation between latencies and current intensity. D. EEP amplitude was correlated with the GSV of reflectance change in the retina. There was a significant positive correlation between intensities of reflectance changes and EEP amplitudes ($r^2 = 0.496$, $P = 0.001$).
doi:10.1371/journal.pone.0092186.g007

similar to that of the reflectance changes induced by the same stimuli [28]. Thus, the reflectance changes investigated in this study represented the hemodynamic responses of the retina and optic nerve to the increased retinal neural activity, which are secondary to the activation of the neural activity of the retina. We suggest that the RCs represent the response of neurovascular coupling and TES might stimulate the neurovascular coupling in the retina and optic nerve.

In conclusion, the intensities of the reflectance changes were dependent on the stimulus parameters of TES. The reflectance changes represent changes of the retinal vessels and optic disc, and these results indicate that TES influenced neurovascular coupling, i.e., RGCs and retinal hemodynamics. More experiments are necessary to determine the retinal neurovascular coupling, i.e., the relationship between the activated RGCs and the retinal hemodynamics. However, we conclude that this imaging technique might be a method to investigate the neurovascular coupling.

Author Contributions

Conceived and designed the experiments: T. Morimoto TF. Performed the experiments: T. Morimoto HK T. Miyoshi YH T. Mihashi YK TF. Analyzed the data: T. Morimoto HK YH T. Mihashi. Contributed reagents/materials/analysis tools: T. Morimoto HK T. Miyoshi YH T. Mihashi YK TF. Wrote the paper: T. Morimoto KN TF.

References

1. Potts AM, Inoue J (1968) The electrically evoked response of the visual system (EER). Invest Ophthalmol 7: 269–278.
2. Potts AM, Inoue J (1969) The electrically evoked response of the visual system (EER) II. Effect of adaptation and retinitis pigmentosa. Invest Ophthalmol 8: 605–613.
3. Miyake Y, Yanagida K, Yagasaki K (1980) Clinical application of EER (electrically evoked response). (1) Analysis of EER in normal subjects. Nippon Ganka Gakkai Zasshi 84: 354–360.
4. Fujikado T, Morimoto T, Matsushita K, Shimojo H, Okawa Y, et al. (2006) Effect of transcorneal electrical stimulation in patients with nonarteritic ischemic optic neuropathy or traumatic optic neuropathy. Jpn J Ophthalmol 50 : 266–273.
5. Inomata K, Shinoda K, Ohde H, Tsunoda K, Hanazono G, et al. (2007) Transcorneal electrical stimulation of retina to treat longstanding retinal artery occlusion. Graefes Arch Clin Exp Ophthalmol 245: 1773–1780.
6. Gall C, Fedorov AB, Ernst L, Borrmann A, Sabel BA (2010) Repetitive transorbital alternating current stimulation in optic neuropathy. NeuroRehabilitation 27: 335–341.
7. Schatz A, Röck T, Naycheva L, Willmann G, Wilhelm B, et al. (2011) Transcorneal electrical stimulation for patients with retinitis pigmentosa: a prospective, randomized, sham-controlled exploratory study. Invest Ophthalmol Vis Sci 23: 4485–4496.
8. Delbeke J, Pins D, Michaux G, Wanet-Defalque MC, Parrini S, et al. (2001) Electrical stimulation of anterior visual pathways in retinitis pigmentosa. Invest Ophthalmol Vis Sci 42: 291–297.
9. Morimoto T, Fukui T, Matsushita K, Okawa Y, Shimojyo H, et al. (2006) Evaluation of residual retinal function by pupillary constrictions and phosphenes using transcorneal electrical stimulation in patients with retinal degeneration. Graefes Arch Clin Exp Ophthalmol 244: 1283–1292.
10. Fujikado T, Morimoto T, Kanda H, Kusaka S, Nakauchi K, et al. (2007) Evaluation of phosphenes elicited by extraocular stimulation in normals and by suprachoroidal-transretinal stimulation in patients with retinitis pigmentosa. Graefes Arch Clin Exp Ophthalmol 245: 1411–1419.
11. Naycheva L, Schatz A, Röck T, Willmann G, Messias A, et al. (2012) Phosphene thresholds elicited by transcorneal electrical stimulation in healthy subjects and patients with retinal diseases. Invest Ophthalmol Vis Sci 53: 7440–7448.
12. Shimazu K, Miyake Y, Watanabe S (1999) Retinal ganglion cell response properties in the transcorneal electrically evoked response of the visual system. Vision Res 39: 2251–2260.
13. Shah HA, Montezuma SR, Rizzo JF 3rd (2006) In vivo electrical stimulation of rabbit retina: effect of stimulus duration and electrical field orientation. Exp Eye Res 83: 247–254.
14. Knighton RW (1975) An electrically evoked slow potential of the frog's retina. I. Properties of response. J Neurophysiol.; 38(1): 185–97.
15. Grinvald A, Lieke E, Frostig RD, Gilbert CD, Wiesel TN (1986) Functional architecture of cortex revealed by optical imaging of intrinsic signals. Nature 324: 361–364.
16. Frostig RD, Lieke EE, Ts'o DY, Grinvald A (1990) Cortical functional architecture and local coupling between neuronal activity and the microcirculation revealed by in vivo high-resolution optical imaging of intrinsic signals. Proc Natl Acad Sci USA 87: 6082–6086.
17. Ts'o DY, Frostig RD, Lieke EE, Grinvald A (1990) Functional organization of primate visual cortex revealed by high resolution optical imaging. Science 249: 417–420.
18. Fukuda M, Rajagopalan UM, Homma R, Matsumoto M, Nishizaki M, et al. (2005) Localization of activity-dependent changes in blood volume to submillimeter-scale functional domains in cat visual cortex. Cerebral Cortex 15: 823–833.
19. Cohen LB (1973) Changes in neuron structure during action potential propagation and synaptic transmission. Physiol Rev 53: 373–418.
20. Tsunoda K, Oguchi Y, Hanazono G, Tanifuji M (2004) Mapping cone- and rod- induced retinal responsiveness in macaque retina by optical imaging. Invest Ophthalmol Vis Sci 45: 3820–3826.
21. Abràmoff MD, Kwon YH, Ts'o D, Soliz P, Zimmerman B, et al. (2006) Visual stimulus-induced changes in human near-infrared fundus reflectance. Invest Ophthalmol Vis Sci 47: 715–721.
22. Okawa Y, Fujikado T, Miyoshi T, Sawai H, Kusaka S, et al. (2007) Optical imaging to evaluate retinal activation by electrical currents using suprachoroidal–transretinal stimulation. Invest Ophthalmol Vis Sci 48: 4777–4784.
23. Hanazono G, Tsunoda K, Shinoda K, Tsubota K, Miyake Y, et al. (2007) Intrinsic signal imaging in macaque retina reveals different types of flash-induced light reflectance changes of different origins. Invest Ophthalmol Vis Sci 48: 2903–2912.
24. Inomata K, Tsunoda K, Hanazono G, Kazato Y, Shinoda K, et al. (2008) Distribution of retinal responses evoked by transscleral electrical stimulation detected by intrinsic signal imaging in macaque monkeys. Invest Ophthalmol Vis Sci 49: 2193–2200.
25. Hanazono G, Tsunoda K, Kazato Y, Tsubota K, Tanifuji M (2008) Evaluating neural activity of retinal ganglion cells by flash-evoked intrinsic signal imaging in macaque retina. Invest Ophthalmol Vis Sci 49: 4655–4663.
26. Schallek J, Li H, Kardon R, Kwon Y, Abramoff M, et al. (2009) Stimulus-evoked intrinsic optical signals in the retina: spatial and temporal characteristics. Invest Ophthalmol Vis Sci 50: 4865–4872.
27. Schallek J, Kardon R, Kwon Y, Abramoff M, Soliz P, et al. (2009) Stimulus-evoked intrinsic optical signals in the retina: pharmacologic dissection reveals outer retinal origins. Invest Ophthalmol Vis Sci 50: 4873–4880.
28. Tsunoda K, Hanazono G, Inomata K, Kazato Y, Suzuki W, et al. (2009) Origins of retinal intrinsic signals: a series of experiments on retinas of macaque monkeys. Jpn J Ophthalmol 53: 297–314.
29. Ts'o D, Schallek J, Kwon Y, Kardon R, Abramoff M, et al. (2009) Noninvasive functional imaging of the retina reveals outer retinal and hemodynamic intrinsic optical signal origins. Jpn J Ophthalmol 53: 334–344.
30. Schallek J, Ts'o D (2011) Blood contrast agents enhance intrinsic signals in the retina: evidence for an underlying blood volume component. Invest Ophthalmol Vis Sci 52: 1325–1335.
31. Mihashi T, Okawa Y, Miyoshi T, Kitaguchi Y, Hirohara Y, et al. (2011) Comparing retinal reflectance changes elicited by transcorneal electrical retinal stimulation with those of optic chiasma stimulation in cats. Jpn J Ophthalmol 55: 49–56.
32. Roy CS, Sherrington CS (1890) On the regulation of the blood supply of the brain. J. Physiol 11: 85–108.
33. Riva CE, Logean E, Falsini B (2005) Visually evoked hemodynamical response and assessment of neurovascular coupling in the optic nerve and retina. Prog Retin Eye Res 24: 183–215.
34. Riva CE, Harino S, Shonat RD, Petrig BL (1991) Flicker evoked increase in optic nerve head blood flow in anesthetized cats. Neurosci Lett 128: 291–296.
35. Riva CE, Cranstoun SD, Petrig BL (1996) Effect of decreased ocular perfusion pressure on blood flow and the flicker-induced flow response in the cat optic nerve head. Microvasc Res 52: 258–269.
36. Kurimoto T, Oono S, Oku H, Tagami Y, Kashimoto R, et al. (2010) Transcorneal electrical stimulation increases chorioretinal blood flow in normal human subjects. Clin Ophthalmol 4: 1441–1446.